

CP Violation and Mixing in Technicolor Models

Adam Martin* and Kenneth Lane†

Department of Physics, Boston University
590 Commonwealth Avenue, Boston, Massachusetts 02215

November 2, 2018

Abstract

Vacuum alignment in technicolor models provides an attractive origin for the quarks' CP violation and, possibly, a natural solution for the strong-CP problem of QCD. We discuss these topics in this paper. Then we apply them to determine plausible mixing matrices for left and right-handed quarks. These matrices determine the Cabibbo-Kobayashi-Maskawa matrix as well as new mixing angles and phases that are observable in extended technicolor (ETC) and topcolor (TC2) interactions. We determine the contributions of these new interactions to CP-violating and mixing observables in the K^0 , B_d and B_s systems. Consistency with mixing and CP violation in the K^0 system requires assuming that ETC interactions are electroweak generation conserving even if technicolor has a walking gauge coupling. Large ETC gauge boson masses and small intergenerational mixing then result in negligibly small ETC contributions to B -meson mixing and CP violation and to $\text{Re}(\epsilon'/\epsilon)$. We confirm our earlier strong lower bounds on TC2 gauge boson masses from B_d - \bar{B}_d mixing. We then pay special attention to the possibility that current experiments indicate a deviation from standard model expectations of the values of $\sin 2\beta$ measured in $B_d \rightarrow J/\psi K_S$, ϕK_S , $\eta' K_S$, and πK_S , studying the ability of TC2 to account for these. We also determine the TC2 contribution to ΔM_{B_s} and to $\text{Re}(\epsilon'/\epsilon)$, and find them to be appreciable.

*aomartin@bu.edu

†lane@bu.edu

1. Introduction and Overview

In this paper we study predictions of topcolor-assisted technicolor models for CP violation in the K^0 and B^0 systems. We are particularly interested in determining whether these or similar models with CP-violating flavor-changing neutral currents can account for the apparent discrepancies with standard model predictions of the parameters measured in $B_d \rightarrow J/\psi K_S$, ϕK_S , $\eta' K_S$ and πK_S :

$$\begin{aligned}
\sin 2\beta_{J/\psi K_S} &= +0.72 \pm 0.05 & [1] \\
\sin 2\beta_{\phi K_S} &= +0.50 \pm 0.25 & (\text{Babar } [2]) \\
\sin 2\beta_{\phi K_S} &= +0.06 \pm 0.33 & (\text{Belle } [3]) \\
\sin 2\beta_{\eta' K_S} &= +0.27 \pm 0.21 & [4] \\
\sin 2\beta_{\pi K_S} &= +0.48^{+0.38}_{-0.47} \pm 0.11 & [5]
\end{aligned} \tag{1}$$

Topcolor-assisted technicolor (TC2) is the most fully-developed *dynamical* description of electroweak and flavor physics (for recent reviews, see Refs. [6] and [7]). It consists of strong technicolor (TC) and topcolor gauge interactions that induce spontaneous breakdown of electroweak $SU(2) \otimes U(1)$ symmetry to $U(1)_{EM}$ and a large top quark condensate $\langle \bar{t}t \rangle \sim (100 \text{ GeV})^3$ and mass $m_t \simeq 170 \text{ GeV}$. The strong gauge groups, plus color and at least part of electroweak $U(1)$, are embedded in an extended technicolor (ETC) gauge group G_{ETC} [8] which, when broken at high energies, provides the 5 MeV to 5 GeV hard masses of all standard model fermions, including the top quark. The masses of ETC gauge bosons range from $M_{ETC} \simeq 10\text{--}50 \text{ TeV}$ for $m_q(M_{ETC}) \simeq 5 \text{ GeV}$ up to $M_{ETC} \simeq 2000\text{--}20,000 \text{ TeV}$ for $m_q(M_{ETC}) \simeq 5 \text{ MeV}$.¹ Such large ETC masses for the light quarks are necessary to adequately suppress their CP-conserving and violating $|\Delta S| = 2$ interactions. Reasonable quark masses are then possible because of the “walking” technicolor gauge coupling [9, 10, 11, 12] that strongly enhances the technifermion condensate $\langle \bar{T}T \rangle_{ETC}$.

In TC2 models, the large top, but not bottom, condensate and mass is due to $SU(3)_1 \otimes U(1)_1$ gauge interactions which are strong near 1 TeV [13]. The $SU(3)_1$ interaction is t - b symmetric while $U(1)_1$ couplings are t - b asymmetric.² In particular, the $U(1)_1$ hypercharges of t and b must satisfy $Y_{1Lt}Y_{1Rt} > 0$ and, probably, $Y_{1Lb}Y_{1Rb} < 0$ (see Sect. 4). This makes these forces supercritical for breaking the top quark chiral symmetry, but subcritical for bottom.³ There are weaker $SU(3)_2 \otimes U(1)_2$ gauge interactions in which light quarks (and leptons) may or may not participate.

¹Appendix A contains our estimates of M_{ETC}/g_{ETC} in generic TC2 models with walking technicolor.

²Electroweak $SU(2)$ and $U(1)_{1,2}$ commute.

³We assume throughout this paper that the effective $U(1)_1$ coupling should be strong, at least for the top and bottom quarks, so that the $SU(3)_1$ coupling does not need to be fine-tuned for top condensation. This raises the concern that the $U(1)_1$ coupling has a Landau pole at low energy [14]. One resolution of this difficulty is that the embedding of $U(1)_1$ and other TC2 gauge groups into G_{ETC} — necessary to avoid an axion [8] — occurs at a low enough energy to forestall the Landau pole.

For TC2 to be consistent with precision measurements of the Z^0 [15], the two $U(1)$'s must be broken to weak hypercharge $U(1)_Y$ at an energy somewhat higher than 1 TeV by electroweak-singlet condensates [16]. This breaking results in a heavy color-singlet Z' boson which plays a central role in this paper. The two $SU(3)$'s are broken at 1 TeV to their diagonal $SU(3)_C$ subgroup — ordinary color. A massive octet of “colorons”, V_8 , mediate the broken topcolor $SU(3)$ interactions.

There are two variants of TC2: The “standard” version, which we denote STC2 [13], in which only the third generation quarks are $SU(3)_1$ triplets. The third generation quarks also transform under $U(1)_1$. *Whether the lighter two quark generations also transform under $U(1)_1$ is a model-dependent question. In this paper we assume that they do.* Indeed, in some models, $U(1)_1$ anomaly cancellation may require it [16]. In STC2 strongly-coupled flavor-changing neutral current (FCNC) interactions are mediated by both V_8 and Z' exchange.⁴ In order that they not be prohibitively large for the light quarks, the first two generations must have flavor-symmetric $U(1)_1$ hypercharges, i.e., for the electroweak eigenstates,

$$\begin{aligned} Y_{1Lu} &= Y_{1Ld} = Y_{1Lc} = Y_{1Ls} , \\ Y_{1Ru} &= Y_{1Rc}, \quad Y_{1Rd} = Y_{1Rs} . \end{aligned} \tag{2}$$

The other variant is the “flavor-universal” version, FUTC2 [17, 18]. There, all quarks are $SU(3)_1$ triplets. The third generation quarks transform under $U(1)_1$ and we assume again that the light generations do too. In FUTC2, only Z' exchange induces new FCNC interactions. Therefore, the $U(1)_1$ hypercharges of light quarks must satisfy Eq. (2) here as well. We consider both TC2 variants in this paper.

In Sect. 2 we review vacuum alignment in technicolor theories and show how this determines CP violation in quark interactions. Vacuum alignment is the process in which ETC and TC2 interactions lift the degeneracy of the infinity of vacua associated with spontaneous breaking of technifermion and quark chiral symmetries. It can induce CP violation in a theory which is superficially CP invariant. This leads to a new, natural scenario for solving the strong-CP problem of QCD.⁵ Alignment generates the matrices $Q_{L,R} = (U, D)_{L,R}$ that rotate left and right-handed up and down quarks from the electroweak basis to the mass-eigenstate one. The Cabibbo-Kobayashi-Maskawa (CKM) matrix is $V = U_L^\dagger D_L$. Observable CP-violating phases appear in the ordinary weak interactions through V and in the TC2 and ETC interactions through $Q_{L,R}$. We review and update general constraints on the form of the alignment matrices in Sect. 2.

In Sect. 3 we describe the TC2 and ETC interactions we use for B^0 and K^0 studies in later sections. Here we show how the quark alignment matrices enter these interactions. We also discuss an important assumption we must make for ETC interactions, namely, that they are electroweak generation conserving. In Sect. 4 we discuss the main constraints on ETC and TC2 that arise from the requirement that TC2 causes no quark other than the top to

⁴Of course, ETC interactions induce FCNC effects as well.

⁵Some of the material presented in Sect. 2 appeared in the conference proceedings Refs. [19, 20, 7]

condense, and from neutral meson mixing and CP violation. Mixing of B_d and \bar{B}_d leads to lower bounds on M_{V_8} and $M_{Z'}$. We confirm the bounds found earlier in Ref. [21], and we are in some disagreement with a later study by Simmons [22]. In Sect. 5 we present the formalism for calculating the TC2 contributions to $B_d \rightarrow XK_S$. Because of our assumption of electroweak generation conservation, the ETC contributions are negligible. Section 6 is a brief review of the definition of the *experimental* $\sin 2\beta_{\text{eff}}$, as opposed to the standard model value, $(\sin 2\beta)_{SM} = \sin(2 \arg(V_{td}^*))$, where V_{td} is the CKM matrix element.

Section 7 contains our main results. They are based on three “models” of the quark mass matrix that are inspired by the CP-violation scenario described in Sect. 2. Once the mass matrices are written down, the alignment matrices $Q_{L,R}$ are determined. We use these to compare the predictions of TC2 with experiment for $B_d \rightarrow J/\psi K_S$, ϕK_S , $\eta' K_S$ and πK_S . We also calculate the influence of TC2 on $x_s = \Delta M_{B_s}/\Gamma_{B_s}$ and $\text{Re}(\epsilon'/\epsilon)$. Our main conclusions are these: (1) If D_R is 2×2 by 1×1 block-diagonal — as *may* be necessary to avoid excessive B_d – \bar{B}_d mixing, both TC2 variants predict that the same value of $\sin 2\beta$ is measured in all these processes and that this value is the one expected in the standard model — even though TC2 may contribute appreciably to the decay amplitudes. (2) If D_R is not block-diagonal, the value of $\sin 2\beta$ extracted from $B_d \rightarrow J/\psi K_S$ is the standard model expectation, but other $B_d \rightarrow XK_S$ decays may lead to different values and even fit the central values of current measurements.⁶ We find that TC2 can account for discrepancies as large as those in the central values of, say, the current Belle measurement, but this typically requires large $U(1)_1$ hypercharges, especially in the FUTC2 variant. These are worrisome because they suggest the $U(1)_1$ coupling has a Landau pole at relatively low energies [14]. This problem is less pronounced with STC2 than with FUTC2 because the latter variant has only the Z' to influence the decays. (3) Depending on the mixing angles in the $D_{L,R}$ alignment matrices, we find that TC2 (plus the standard model) can produce values of x_s ranging from the experimental lower bound of about 20 up to several hundred. (4) For the mass matrix models we considered, the standard model contributions to $\text{Re}(\epsilon'/\epsilon)$ happened to be about 1/4 the measured value. With Z' and V_8 masses consistent with B_d – \bar{B}_d mixing, the TC2 contribution then can account for the remainder so long as we require $Y_{1Ru} \cong Y_{1Rd}$.

2. Vacuum Alignment and CP Violation in Technicolor

Quark CP violation in technicolor models is a consequence of “vacuum alignment” [24, 25, 26]. The idea is simple: In technicolor, large flavor/chiral symmetries of the technifermions and quarks are spontaneously broken when their dynamics become strong. This leads to an infinity of degenerate vacua. The degeneracy is at least partly lifted by ETC interactions which explicitly break all global flavor symmetries. Vacuum alignment is the process of finding the (perturbative) ground state which minimizes the expectation value of the chiral-

⁶Burdman has recently carried out similar studies [23] in which he considered the effects of warped extra dimensions and of topcolor V_8 (but not Z') exchange.

symmetry breaking Hamiltonian \mathcal{H}' . This Hamiltonian is generated by the exchange of ETC gauge bosons and it is natural to assume that it is CP-conserving. As Dashen first showed, however, the ground state $|\Omega\rangle$ which minimizes $\langle\Omega|\mathcal{H}'|\Omega\rangle$ may not respect the same CP symmetry that \mathcal{H}' does. In this case, CP is spontaneously broken and $|\Omega\rangle$ is discretely degenerate.⁷ As we discuss below, this scenario offers the possibility of naturally solving the strong-CP problem of QCD — without an axion and without a massless up quark.

New CP-violating phases are introduced into the K^0 and B^0 decay amplitudes by quark-alignment matrices $Q_{L,R}$. To understand how the $Q_{L,R}$ are determined, we briefly describe vacuum alignment in technicolor theories. Readers familiar with this material can skip to Eq. (12).

As in Ref. [27], we consider simple models in which a single kind of technifermion interacts with itself and with quarks via ETC interactions. Leptons are ignored. There are N doublets of these technifermions, $T_{L,RI} = (\mathcal{U}_{L,RI}, \mathcal{D}_{L,RI})$, $I = 1, 2, \dots, N$, all assumed to transform according to the fundamental representation of the TC gauge group $SU(N_{TC})$. They are ordinary color-singlets.⁸ There are three generations of $SU(3)_C$ triplet quarks $q_{L,Ri} = (u_{L,Ri}, d_{L,Ri})$, $i = 1, 2, 3$. Left-handed fermions are electroweak $SU(2)$ doublets and right-handed ones are singlets. Here and below, we exhibit only flavor, not TC and QCD, indices.

The joint T - q chiral flavor group of our model is $G_f = [SU(2N)_L \otimes SU(2N)_R]_T \otimes [SU(6)_L \otimes SU(6)_R]_q$.⁹ When the TC and QCD couplings reach critical values, these symmetries are spontaneously broken to $S_f = SU(2N) \otimes SU(6)$. Rather than fix the symmetry-breaking Hamiltonian and vary over the ground states, it is convenient to work in a “standard vacuum” $|\Omega\rangle$ whose symmetry group is the vectorial $SU(2N)_V \otimes SU(6)_V$, and chirally rotate \mathcal{H}' . Fermion bilinear condensates in $|\Omega\rangle$ have the simple form

$$\begin{aligned}\langle\Omega|\bar{\mathcal{U}}_{LI}\mathcal{U}_{RJ}|\Omega\rangle &= \langle\Omega|\bar{\mathcal{D}}_{LI}\mathcal{D}_{RJ}|\Omega\rangle = -\delta_{IJ}\Delta_T \\ \langle\Omega|\bar{u}_{Li}u_{Rj}|\Omega\rangle &= \langle\Omega|\bar{d}_{Li}d_{Rj}|\Omega\rangle = -\delta_{ij}\Delta_q.\end{aligned}\tag{3}$$

Here, $\Delta_T \simeq 2\pi F_T^3$ and $\Delta_q \simeq 2\pi f_\pi^3$ where $F_T = 246 \text{ GeV}/\sqrt{N}$ is the technipion decay constant.¹⁰

⁷We are aware that spontaneous CP violation at 1 TeV implies a significant domain-wall problem. Should this mechanism prove successful, we are confident that cosmologists will find a way to eliminate the problem.

⁸This is not correct for TC2 where some technifermions are expected to be triplets under $SU(3)_1$ or $SU(3)_2$. This complication is not important for the analysis of K^0 and B^0 decays in later sections.

⁹The fact that heavy quark chiral symmetries cannot be treated by chiral perturbative methods will be addressed below. We have excluded anomalous $U_A(1)$ ’s strongly broken by TC and color instanton effects. Therefore, alignment matrices must be unimodular.

¹⁰In TC2 models with topcolor breaking by technifermion condensation [16], $N \sim 10$. This large N raises the question of technicolor’s contribution to precisely measured electroweak quantities such as S , T , and U . Calculations that show technicolor to be in conflict with precision measurements have been based on the assumption that technicolor dynamics are just a scaled-up version of QCD [28, 29, 30]. However, this cannot be because of the walking TC gauge coupling [7]. In walking technicolor there must be something like a tower of spin-one technihadrons reaching almost to the ETC scale, and these states contribute significantly

We write the ETC Hamiltonian in the phenomenological four-fermion form (sum over repeated flavor indices) ¹¹

$$\begin{aligned}
\mathcal{H}' &\equiv \mathcal{H}'_{TT} + \mathcal{H}'_{Tq} + \mathcal{H}'_{qq} \\
&= \Lambda_{IJKL}^{TT} \bar{T}_{LI} \gamma^\mu T_{LJ} \bar{T}_{RK} \gamma_\mu T_{RL} + \Lambda_{IijJ}^{Tq} \bar{T}_{LI} \gamma^\mu q_{Li} \bar{q}_{Rj} \gamma_\mu T_{RJ} + \text{h.c.} \\
&+ \Lambda_{ijkl}^{qq} \bar{q}_{Li} \gamma_\mu q_{Lj} \bar{q}_{Rk} \gamma_\mu q_{Rl} + \text{LL and RR terms.}
\end{aligned} \tag{4}$$

Here, the fields $T_{L,Ri}$ and $q_{L,Ri}$ stand for all $2N$ technifermions and six quarks, respectively. The Λ coefficients are $\mathcal{O}(g_{ETC}^2/M_{ETC}^2)$ times ETC boson mixing factors and group theoretical factors for the broken generators of ETC. The LL and RR terms do not enter vacuum alignment, but they can be important for quark FCNC interactions. The Λ 's may have either sign. In all calculations, we must choose the Λ 's to avoid very light pseudoGoldstone bosons (e.g., axions). Hermiticity of \mathcal{H}' requires $(\Lambda_{IJKL}^{TT})^* = \Lambda_{JILK}^{TT}$, etc. Assuming, for simplicity, that color and technicolor are embedded in a simple nonabelian ETC group, the instanton angles θ_{TC} and θ_{QCD} are equal. Without loss of generality, we may work in vacua in which they are zero. Then strong-CP violation in QCD is characterized by $\bar{\theta}_q = \arg \det(M_q)$, where M_q is the quark mass matrix. The assumption of time-reversal invariance for this theory before any potential breaking via vacuum alignment then means that all the Λ 's are *real* and so $\Lambda_{IJKL}^{TT} = \Lambda_{JILK}^{TT}$, etc.

Vacuum alignment now proceeds by minimizing the expectation value of \mathcal{H}' rotated by elements of G_f/S_f . Make the transformations $T_{L,R} \rightarrow W_{L,R} T_{L,R}$ and $q_{L,R} \rightarrow Q_{L,R} q_{L,R}$, where $W_{L,R} \in SU(2N)_{L,R}$ and $Q_{L,R} \in SU(6)_{L,R}$. Then

$$\begin{aligned}
\mathcal{H}'(W, Q) &= \mathcal{H}'_{TT}(W_L, W_R) + \mathcal{H}'_{Tq}(W, Q) + \mathcal{H}'_{qq}(Q_L, Q_R) \\
&= \Lambda_{IJKL}^{TT} \bar{T}_{LI'} W_{L'I'}^\dagger \gamma^\mu W_{LJJ'} T_{LJ'} \bar{T}_{RK'} W_{RK'}^\dagger \gamma^\mu W_{RLL'} T_{RL'} + \dots
\end{aligned} \tag{5}$$

Since T and q transform according to complex representations of their respective color groups, the vacuum energy to be minimized has the form

$$\begin{aligned}
E(W, Q) &\equiv \langle \Omega | \mathcal{H}'(W, Q) | \Omega \rangle = E_{TT}(W) + E_{Tq}(W, Q) + E_{qq}(Q) \\
&= -\Lambda_{IJKL}^{TT} W_{JK} W_{LI}^\dagger \Delta_{TT} - \left(\Lambda_{IijJ}^{Tq} Q_{ij} W_{JI}^\dagger + \text{c.c.} \right) \Delta_{Tq} - \Lambda_{ijkl}^{qq} Q_{jk} Q_{li}^\dagger \Delta_{qq} \\
&= -\Lambda_{IJKL}^{TT} W_{JK} W_{LI}^\dagger \Delta_{TT} (1 + \rho).
\end{aligned} \tag{6}$$

The factor $\rho = \mathcal{O}(10^{-11})$ is explained below. Vacuum alignment must preserve electric charge conservation, and so the minimum of E occurs in the subspace of block-diagonal alignment

to the integrals over spectral functions involved in calculating S , T , and U . Therefore, in the absence of detailed experimental knowledge of this spectrum, including the spacing between states and their coupling to the electroweak currents, it is not possible to calculate S , T , U reliably.

¹¹We assume that ETC interactions commute with electroweak $SU(2)$, though not with $U(1)$ nor color $SU(3)$. All fields in Eq. (4) are electroweak, not mass, eigenstates. In writing \mathcal{H}' , we assume that topcolor breaking to $SU(3)_C \otimes U(1)_Y$ has occurred. Broken topcolor interactions can always be put in the form of terms appearing in \mathcal{H}' .

matrices

$$W_{L,R} = \begin{pmatrix} W_{L,R}^U & 0 \\ 0 & W_{L,R}^D \end{pmatrix}; \quad Q_{L,R} = \begin{pmatrix} U_{L,R} & 0 \\ 0 & D_{L,R} \end{pmatrix}. \quad (7)$$

Note that time-reversal invariance of the unrotated Hamiltonian \mathcal{H}' implies that $E(W, Q) = E(W^*, Q^*)$. Hence, spontaneous CP violation occurs if the solutions W_0, Q_0 to the minimization problem are not real (up to an overall \mathcal{Z}_N phase).

In Eq. (6), Δ_{TT} , Δ_{Tq} and Δ_{qq} are *positive* four-fermion condensates in the standard vacuum, $|\Omega\rangle$. They are renormalized at the appropriate M_{ETC} scale and are given approximately by

$$\begin{aligned} \Delta_{TT} &\simeq (\Delta_T(M_{ETC}))^2 \\ \Delta_{Tq} &\simeq \Delta_T(M_{ETC}) \Delta_q(M_{ETC}) \\ \Delta_{qq} &\simeq (\Delta_q(M_{ETC}))^2. \end{aligned} \quad (8)$$

In walking technicolor (see Appendix A)

$$\Delta_T(M_{ETC}) \lesssim (M_{ETC}/\Lambda_{TC}) \Delta_T(\Lambda_{TC}) = 10^2 - 10^4 \times \Delta_T(\Lambda_{TC}). \quad (9)$$

In QCD, however,¹²

$$\Delta_q(M_{ETC}) \simeq (\log(M_{ETC}/\Lambda_{QCD}))^{\gamma_m} \Delta_q(\Lambda_{QCD}) \simeq \Delta_q(\Lambda_{QCD}), \quad (10)$$

where the anomalous dimension γ_m of $\bar{q}q$ is small.¹³ Thus,

$$\rho = \frac{\Delta_{Tq}(M_{ETC})}{\Delta_{TT}(M_{ETC})} \simeq \frac{\Delta_{qq}(M_{ETC})}{\Delta_{Tq}(M_{ETC})} \simeq \frac{\Lambda_{TC}}{M_{ETC}} \left(\frac{f_\pi}{F_T} \right)^3 \lesssim 10^{-11} \quad (11)$$

for $F_T \simeq 100$ GeV. This ratio is 10^2 – 10^4 times smaller than it is in a technicolor theory in which the coupling does not walk.

The last line of Eq. (6) makes clear that we should first minimize the energy E_{TT} in the technifermion sector. Because W may be assumed block-diagonal, E_{TT} factorizes into two terms, $E_{UU} + E_{DD}$, in which W_U and W_D may each be taken unimodular. We may then minimize separately in the \mathcal{U} and \mathcal{D} sectors. This determines $W_0 = (W_0^U, W_0^D)$, and as we shall see, $\bar{\theta}_q$, up to corrections of $\mathcal{O}(10^{-11})$ from the quark sector.¹⁴ This result is then fed

¹²In TC2, Eq. (10) must be modified to account for the embedding of $SU(3)_C$ into $SU(3)_1 \otimes SU(3)_2$ and the latter group's embedding into G_{ETC} .

¹³We shall assume that γ_m remains small in FUTC2, even though quarks have strong $SU(3)_1$ interactions there.

¹⁴Two other sorts of corrections need to be studied. The first are higher-order ETC and electroweak contributions to E_{TT} . The electroweak ones are naively $\mathcal{O}(10^{-7})$, much too large for $\bar{\theta}_q$. The second are due to $\bar{T}t\bar{t}T$ terms in E_{Tq} which may be important if the top condensate is large. I thank J. Donoghue and S. L. Glashow for emphasizing the potential importance of these corrections.

into E_{Tq} which is minimized to determine Q_0 — and the nature of *weak* CP violation in the quark sector — up to corrections which are also $\mathcal{O}(10^{-11})$.

In Ref. [27], it was shown that minimizing E_{TT} leads to three possibilities for the phases in W . (We drop its subscript “0” from now on.) Let us write $W_{IJ} = |W_{IJ}| \exp(i\phi_{IJ})$. Consider an individual term, $-\Lambda_{IJKL}^{TT} W_{JK} W_{LI}^\dagger \Delta_{TT}$, in E_{TT} . If $\Lambda_{IJKL}^{TT} > 0$, this term is least if $\phi_{IL} = \phi_{JK}$; if $\Lambda_{IJKL}^{TT} < 0$, it is least if $\phi_{IL} = \phi_{JK} \pm \pi$. We say that $\Lambda_{IJKL}^{TT} \neq 0$ *links* ϕ_{IL} and ϕ_{JK} , and tends to align (or antialign) them. Of course, the constraints of unitarity may partially or wholly frustrate this alignment. The three cases for the phases ϕ_{IJ} are:

1. The phases are all unequal, irrational multiples of π that are random except for the constraints of unitarity and unimodularity.
2. All of the phases are equal to the same integer multiple of $2\pi/N \pmod{\pi}$. This may occur when all phases are linked and aligned, and the value $2\pi/N$ is a consequence of the unimodularity of W_U and W_D . In this case we say that the phases are “rational”.
3. Several groups of phases may be linked among themselves but not with others. The phases may then be only partially aligned and they take on *various* rational multiples of π/N' for one or more integers N' from 1 to N .

As far as we know, such nontrivial rational phases (i.e., $\neq 0, \pi, \pi/2$) occur naturally only in ETC theories. They are a consequence of E_{TT} being quadratic, not linear, in W and of the instanton-induced unimodularity constraints on W . Given these three possibilities, we now investigate the quarks’ CP violation.

There are two kinds of CP violation. Weak CP violation enters the standard weak interactions through the CKM phase δ_{13} and the ETC and TC2 interactions through physically observable combinations of phases in the quark alignment matrices $Q_{L,R}$. Strong CP violation, which can produce electric dipole moments 10^{10} times larger than the experimental bound, is a consequence of instantons [31]. No theory of the origin of CP violation is complete which does not eliminate strong CP violation. Resolving this problem amounts to achieving $\bar{\theta}_q \lesssim 10^{-10}$ *naturally*. Let us see how this might happen in technicolor.

The “primordial” quark mass matrix element $(\mathcal{M}_q)_{ij}$, the coefficient of the bilinear $\bar{q}'_{Ri} q'_{Lj}$ of quark *electroweak* eigenstates, is generated by ETC interactions and is given by¹⁵

$$(\mathcal{M}_q)_{ij} = \sum_{I,J} \Lambda_{IijJ}^{Tq} W_{JI}^\dagger \Delta_T(M_{ETC}) \quad (q, T = u, U \text{ or } d, D). \quad (12)$$

The Λ_{IijJ}^{Tq} are real ETC couplings of order $(10^2\text{--}10^4 \text{ TeV})^{-2}$ (see Appendix A). Since the quark alignment matrices $Q_{L,R}$ which diagonalize \mathcal{M}_q to M_q are unimodular, $\arg \det(M_q) = \arg \det(\mathcal{M}_q) = \arg \det(\mathcal{M}_u) + \arg \det(\mathcal{M}_d)$. Therefore, strong CP violation depends *entirely*

¹⁵The matrix element $(\mathcal{M}_u)_{tt}$ arises almost entirely from the TC2-induced condensation of top quarks. We assume that $\langle \bar{t}t \rangle$ and $(\mathcal{M}_u)_{tt}$ are real in the basis in which $\theta_{QCD} = 0$. Since technicolor, color, and topcolor groups are embedded in ETC, all CP-conserving condensates are real in this basis.

on the character of vacuum alignment in the technifermion sector — the phases ϕ_{IJ} of W — and by how the ETC factors Λ_{IjJ}^{Tq} map these phases into the $(\mathcal{M}_q)_{ij}$.

If the ϕ_{IJ} are random irrational phases, $\bar{\theta}_q$ could vanish only by the most contrived, unnatural adjustment of the Λ^{Tq} and, so, this case generically exhibits strong CP violation. If all $\phi_{IJ} = 2m\pi/N \pmod{\pi}$, then all elements of \mathcal{M}_u have the same phase, as do all elements of \mathcal{M}_d . Then, $U_{L,R}$ and $D_{L,R}$ will be real orthogonal matrices, up to an overall phase. There may be strong CP violation, but there will no weak CP violation in any interaction.

There remains the possibility, which we assume henceforth, that the ϕ_{IJ} are different rational multiples of π . Then, strong CP violation will be absent *if* the Λ^{Tq} map these phases onto the primordial mass matrix so that (1) each element $(\mathcal{M}_q)_{ij}$ has a rational phase *and* (2) these add to zero in $\arg \det(\mathcal{M}_q)$. In the absence of an explicit ETC model, we do not know whether this can happen, but we see no reason it cannot. For example, there may be just one pair (IJ) for which $\Lambda_{IjJ}^{Tq} \neq 0$ for fixed (ij) . An ETC model which achieves such a phase mapping would solve the strong CP problem, i.e., $\bar{\theta}_q \lesssim 10^{-11}$, without an axion and without a massless up quark. This is, in effect, a “natural fine-tuning” of phases in the quark mass matrix: rational phase solutions are stable against substantial changes in the nonzero Λ^{TT} . There is, of course, no reason weak CP violation will not occur in this scenario.

Determining the quark alignment matrices $Q_{L,R}$ begins with minimizing the vacuum energy (using $\Delta_{Tq} \cong \Delta_T \Delta_q$)

$$E_{Tq}(Q) \cong -\text{Tr}(\mathcal{M}_q Q + \text{h.c.}) \Delta_q(M_{ETC}) \quad (13)$$

to find $Q = Q_L Q_R^\dagger$. When $\bar{\theta}_q = 0$, this is equivalent to making the mass matrix diagonal, real, and positive. Whether or not $\bar{\theta}_q = 0$, the matrix $\mathcal{M}_q Q$ is hermitian up to the identity matrix [24],

$$\mathcal{M}_q Q - Q^\dagger \mathcal{M}_q^\dagger = i\nu_q 1, \quad (14)$$

where ν_q is the Lagrange multiplier associated with the unimodularity constraint on Q [32], and ν_q vanishes if $\bar{\theta}_q$ does. Therefore, $\mathcal{M}_q Q$ may be diagonalized by the single unitary transformation Q_R and, so,¹⁶

$$M_q \equiv \begin{pmatrix} M_u & 0 \\ 0 & M_d \end{pmatrix} = Q_R^\dagger \mathcal{M}_q Q Q_R = Q_R^\dagger \mathcal{M}_q Q_L. \quad (15)$$

The CKM matrix is $V = U_L^\dagger D_L$. Carrying out the *vectorial* phase changes on $q_{L,Ri}$ required to put V in the standard form with a single CP-violating phase δ_{13} , one obtains [33,

¹⁶Since quark vacuum alignment is based on first order chiral perturbation theory, it is inapplicable to the heavy quarks c, b, t . However, since it just amounts to diagonalizing \mathcal{M}_q when $\bar{\theta}_q = 0$, it correctly determines the quark unitary matrices $U_{L,R}$ and $D_{L,R}$ and the magnitude of strong and weak CP violation.

$$\begin{aligned}
V &\equiv \begin{pmatrix} V_{ud} & V_{us} & V_{ub} \\ V_{cd} & V_{cs} & V_{cb} \\ V_{td} & V_{ts} & V_{tb} \end{pmatrix} \\
&= \begin{pmatrix} c_{12} c_{13} & s_{12} c_{13} & s_{13} e^{-i\delta_{13}} \\ -s_{12} c_{23} - c_{12} s_{23} s_{13} e^{i\delta_{13}} & c_{12} c_{23} - s_{12} s_{23} s_{13} e^{i\delta_{13}} & s_{23} c_{13} \\ s_{12} s_{23} - c_{12} c_{23} s_{13} e^{i\delta_{13}} & -c_{12} s_{23} - s_{12} c_{23} s_{13} e^{i\delta_{13}} & c_{23} c_{13} \end{pmatrix}.
\end{aligned} \tag{16}$$

Here, $s_{ij} = \sin \theta_{ij}$, and the angles θ_{12} , θ_{23} , θ_{13} lie in the first quadrant. Additional CP-violating phases appear in $U_{L,R}$ and $D_{L,R}$; certain linear combinations are observable in the ETC and TC2 interactions. We discuss next the form of \mathcal{M}_u , \mathcal{M}_d and $U_{L,R}$, $D_{L,R}$ imposed by experimental constraints on ETC and TC2.

First, limits on FCNC interactions, especially those contributing to $\Delta M_K = M_{K_L} - M_{K_S}$ and the CP-violation parameter ϵ , require that ETC bosons coupling to the two light generations have masses $M_{ETC}/g_{ETC} \gtrsim 10^3$ TeV (see Ref. [7] for the latest estimates). These can produce quark masses less than about $m_s(M_{ETC}) \simeq 100$ MeV in a walking technicolor theory (see Fig. 12 in Appendix A). We expect similar or smaller masses in the first two rows of $\mathcal{M}_{u,d}$ (except $\mathcal{M}_{cc} \simeq 1$ GeV). Extended technicolor bosons as light as 50–100 TeV are needed to generate $m_b(M_{ETC}) \simeq 4$ GeV. Flavor-changing neutral current interactions mediated by such light ETC bosons must be suppressed by small mixing angles between the third and the first two generations.¹⁷

The most important feature of \mathcal{M}_u is that the TC2 component of $(\mathcal{M}_u)_{tt}$, $\hat{m}_t = 160$ – 170 GeV, is much larger than its other elements, all of which are generated by ETC exchange. In particular, off-diagonal elements in the third row and column of \mathcal{M}_u are expected to be no larger than the 0.01–1.0 GeV associated with m_u and m_c . So, \mathcal{M}_u and $U_{L,R}$ are very nearly block-diagonal with $|U_{L,Rtu_i}| \cong |U_{L,Ru_it}| \cong \delta_{tu_i}$.

There is an argument that the matrix \mathcal{M}_d must have, or nearly have, a triangular texture [16]; also see Ref. [35]: In 1995 Kominis argued that in topcolor models the $SU(3)_1 \otimes U(1)_1$ couplings of the bottom quark are not far from the critical values required for condensation. Consequently, there ought to exist so-called “bottom pions” — relatively light ($\simeq 300$ GeV) scalar bound states of $\bar{t}_L b_R$ and $\bar{b}_L b_R$ that couple strongly ($\propto \hat{m}_t$) to third generation quarks [36]. Bottom pions will induce excessive $B_d - \bar{B}_d$ mixing unless $|D_{Lbd} D_{Rbd}| \lesssim 10^{-7}$. In addition to this, since U_L is block-diagonal, the observed CKM mixing between the first two generations and the third must come from the down sector matrix D_L . These considerations (and the need for flavor symmetry in the two light generations) imply that the \mathcal{M}_d is approximately triangular, with its $d_R, s_R \leftrightarrow b_L$ elements \mathcal{M}_{db} and \mathcal{M}_{sb} much smaller than its $d_L, s_L \leftrightarrow b_R$ elements.

¹⁷We must assume that the ETC interactions \mathcal{H}'_{qq} are electroweak generation conserving to suppress $|\Delta S| = 2$ FCNC interactions adequately. We also assume that the magnitude of Λ_{ijkl}^{qq} is comparable to that of Λ_{iLl}^{Tq} and/or Λ_{jKk}^{Tq} . See Eq. (23) in Sect. 3.

A triangular \mathcal{M}_d was produced in the TC2 models of Refs. [37, 16, 38] by choosing the topcolor $U(1)_1$ charges to forbid ETC interactions that induce the $d_R, s_R \leftrightarrow b_L$ matrix elements $\mathcal{M}_{db}, \mathcal{M}_{sb}$. Then D_R , like $U_{L,R}$, is nearly 2×2 times 1×1 block-diagonal. Although both V_8 and Z' exchange produce FCNC interactions, this constraint plus the approximate flavor symmetry implied by Eq. (2) mean that many interesting FCNC effects arise only from left-handed $\bar{b}'_L b'_L \bar{b}'_L b'_L$ TC2 interactions. Then the magnitudes and phases of the mixing factors are simply related to those of CKM elements (as in Eq. (17) below).

Kominis' argument for near-criticality of b -quark TC2 interactions relied on assuming it had standard-model $U(1)_1$ hypercharges $Y_{1Lb} = 1/6$ and $Y_{1Rb} = -1/3$ and that the $U(1)_1$ coupling is not very strong (to avoid a Landau pole at low energy). As we noted above, however, a strong $U(1)_1$ coupling is needed to avoid fine-tuning the $SU(3)_1$ coupling, while the Landau pole might be avoided if $U(1)_1$ is embedded in G_{ETC} at low enough energy. Thus, we view the existence of bottom pions as arguable at best. For STC2, we shall consider both cases: D_R is block-diagonal and it is not.

In Ref. [22] Simmons pointed out that there may be an amelioration of the bottom pion contribution to $B_d - \bar{B}_d$ mixing in FUTC2. There, all quarks have strong attractive $SU(3)_1$ interactions so that there would be “q-pions” with flavor-symmetric couplings for all the quarks *if* $U(1)_1$ is relatively weak — as Simmons assumed necessary to avoid a Landau pole. Such q-pions would not induce $B_d - \bar{B}_d$ mixing. However, whether or not light quarks transform under $U(1)_1$, the heavy ones do *and* their $U(1)_1$ couplings should not be weak. This ruins the flavor symmetry of q-pions' couplings and Simmons' argument fails. Furthermore, if light quarks do have $U(1)_1$ interactions then, like the bottom quark's, they probably must be repulsive. This calls into question the very existence of *all* q-pions *except* the top pion. In short, the matter of q-pions and their induced $B_d - \bar{B}_d$ mixing is highly uncertain. In FUTC2, even more than in STC2, the argument for \mathcal{M}_d to be triangular and D_R block-diagonal is weak and, like Simmons, we shall not be bound by it.

Because mixing between the third generation and the two lighter ones comes from D_L , in either TC2 variant we have (using $V_{tb} \cong 1$, and independent of the form of D_R)

$$V_{td_i} \cong V_{tb}^* V_{td_i} \cong U_{Lt} D_{Lbb}^* U_{Ltt}^* D_{Lbd_i} \cong D_{Lbb}^* D_{Lbd_i}. \quad (17)$$

This relation is good to 5%. Together with the assumption that D_R is block-diagonal, it was used in Ref. [21] to put limits on the TC2 V_8 and Z' masses from $B_d - \bar{B}_d$ mixing. It was shown there that $M_{V_8}, M_{Z'} \gtrsim 5 \text{ TeV} \gg \hat{m}_t$. This implies that the TC2 gauge couplings must be tuned to within 1% or better of their critical values — an uncomfortably fine tuning in a dynamical theory. For FUTC2, Simmons' q-pion argument and assumption that $U(1)_1$ is relatively weak led her to conclude that this bound could be lowered for the Z' (as well as for the V_8 which does not mediate FCNC interactions). We revisit this question in Sect. 3 and conclude that the bound $M_{V_8, Z'} \gtrsim 5 \text{ TeV}$ generally holds in both TC2 variants.

To calculate the TC2 and ETC contributions to CP-violating parameters in K and B -decays, we generated three representative sets of alignment matrices $U_{L,R}$ and $D_{L,R}$. They were created by carrying out vacuum alignment with a non-hermitian primordial mass matrix

\mathcal{M}_q satisfying $\arg \det(\mathcal{M}_q) = 0$. The first set of alignment matrices (Mass Model 1) has a block-diagonal D_R , as was assumed Ref. [21].¹⁸ Mass Models 2 and 3 have $D_R \sim D_L$. The mass and alignment matrices are presented in Appendix B. As we shall see in Sect. 5, a discrepancy in the value of $\sin 2\beta$ measured in different decays is possible only in models with a non-block-diagonal D_R .

3. TC2 and ETC Interactions

At energies well below $M_{V_8, Z'}$, the effective TC2 current \times current interaction is

$$\mathcal{H}_{TC2} \equiv \mathcal{H}_{Z'} + \mathcal{H}_{V_8} = \frac{g_Y^2}{2M_{Z'}^2} J_{Z'\mu} J_{Z'}^\mu + \frac{g_C^2}{2M_{V_8}^2} J^{A\mu} J_\mu^A, \quad (18)$$

where

$$\begin{aligned} J_{Z'\mu} &= \sum_{\lambda=L,R} \sum_i \left(Y_{1\lambda i} \cot \theta_Y - Y_{2\lambda i} \tan \theta_Y \right) \bar{q}'_{\lambda i} \gamma_\mu q'_{\lambda i}, \\ J_\mu^A &= \sum_{\lambda=L,R} \left(\sum_{i=t,b} A_h - \sum_{i=u,d,s,c} A_l \right) \bar{q}'_{\lambda i} \gamma_\mu \frac{\lambda_A}{2} q'_{\lambda i}. \end{aligned} \quad (19)$$

The primed fields are electroweak eigenstates. The couplings g_Y and g_C are the standard model hypercharge and color couplings, defined in terms of the original $SU(3)$ ($U(1)$) couplings by

$$\begin{aligned} g_C &= \frac{g_1 g_2}{\sqrt{g_1^2 + g_2^2}} \quad ; \quad \frac{g_1}{g_2} = \cot \theta_C \gg 1 \\ g_Y &= \frac{g'_1 g'_2}{\sqrt{g_1'^2 + g_2'^2}} \quad ; \quad \frac{g'_1}{g'_2} = \cot \theta_Y \gg 1 \end{aligned}$$

The $U(1)_1$ and $U(1)_2$ hypercharges $Y_{1\lambda i}$ and $Y_{2\lambda i}$ satisfy the flavor symmetry conditions in Eq. (2) and, of course, $Y_{Li} = Y_{1Li} + Y_{2Li} = 1/6$ and $Y_{Ri} = Y_{1Ri} + Y_{2Ri} = e_i$, the electric charge of q_i . We shall ignore the $Y_{2\lambda i} \tan \theta_Y$ terms in our calculations. The couplings of the heavy and light quarks to the coloron, A_h and A_l , depend on the TC2 model. In STC2, only the third generation couples to the strong $SU(3)_1$, so that $A_h = \cot \theta_C$ and $A_l = \tan \theta_C$. In this case, both $\mathcal{H}_{Z'}$ and \mathcal{H}_{V_8} contain FCNC interactions. In FUTC2, all quarks have the same coupling to the colorons, $A_h = -A_l = \cot \theta_C$, and only $\mathcal{H}_{Z'}$ has FCNC interactions.

Expanding \mathcal{H}_{TC2} for the FUTC2 and STC2 variants, and keeping only the strongly

¹⁸Sets of alignment matrices were created in this way in Refs. [20, 7] to calculate the TC2 and ETC contributions to ϵ .

coupled $U(1)_1$ and $SU(3)_1$ contributions to potential FCNC interactions, we obtain

$$\mathcal{H}_{FU} = \mathcal{H}_{Z'} = \frac{g_Y^2 \cot^2 \theta_Y}{2M_{Z'}^2} \sum_{i,j} \sum_{\lambda_1, \lambda_2=L,R} Y_{\lambda_1 i} Y_{\lambda_2 j} \bar{q}'_{\lambda_1 i} \gamma^\mu q'_{\lambda_1 i} \bar{q}'_{\lambda_2 j} \gamma_\mu q'_{\lambda_2 j}; \quad (20)$$

$$\mathcal{H}_S = \mathcal{H}_{Z'} + \mathcal{H}_{V_8} = \mathcal{H}_{FU} + \frac{g_C^2 \cot^2 \theta_C}{2M_{V_8}^2} \sum_{i,j=t,b} \sum_{\lambda_1, \lambda_2=L,R} \bar{q}'_{\lambda_1 i} \gamma^\mu \frac{\lambda_A}{2} q'_{\lambda_1 i} \bar{q}'_{\lambda_2 j} \gamma_\mu \frac{\lambda_A}{2} q'_{\lambda_2 j}.$$

From now on, we denote $Y_{1\lambda i}$ by $Y_{\lambda i}$. Remember that we assume that all quarks transform nontrivially under the strong $U(1)_1$.

Still assuming that the ETC gauge group commutes with electroweak $SU(2)$, the ETC four-quark interaction to lowest order in G_{ETC}^2 is

$$\begin{aligned} \mathcal{H}_{ETC} \equiv \mathcal{H}'_{qq} = & \Lambda_{ijkl}^{LL} (\bar{u}'_{Li} \gamma^\mu u'_{Lj} + \bar{d}'_{Li} \gamma^\mu d'_{Lj}) (\bar{u}'_{Lk} \gamma^\mu u'_{Ll} + \bar{d}'_{Lk} \gamma^\mu d'_{Ll}) \\ & + (\bar{u}'_{Li} \gamma^\mu u'_{Lj} + \bar{d}'_{Li} \gamma^\mu d'_{Lj}) \left(\Lambda_{ijkl}^{u,LR} \bar{u}'_{Rk} \gamma^\mu u'_{Rl} + \Lambda_{ijkl}^{d,LR} \bar{d}'_{Rk} \gamma^\mu d'_{Rl} \right) \\ & + \Lambda_{ijkl}^{uu,RR} \bar{u}'_{Ri} \gamma^\mu u'_{Rj} \bar{u}'_{Rk} \gamma^\mu u'_{Rl} + \Lambda_{ijkl}^{dd,RR} \bar{d}'_{Ri} \gamma^\mu d'_{Rj} \bar{d}'_{Rk} \gamma^\mu d'_{Rl} \\ & + \Lambda_{ijkl}^{ud,RR} \bar{u}'_{Ri} \gamma^\mu u'_{Rj} \bar{d}'_{Rk} \gamma^\mu d'_{Rl}. \end{aligned} \quad (21)$$

Since the ETC gauge group contains technicolor, color and topcolor, and flavor as commuting subgroups, the flavor currents in \mathcal{H}_{ETC} are color and topcolor singlets. The operators are renormalized at the ETC scale of their Λ -coefficients. Hermiticity and CP-invariance of \mathcal{H}_{ETC} implies that $\Lambda_{ijkl} = \Lambda_{jikl}^* = \Lambda_{ijkl}^*$. When written in terms of mass eigenstate fields $q_{L,Ri} = \sum_j (Q_{L,R}^\dagger)_{ij} q'_{L,Rj}$ with $Q = U, D$, an individual term in \mathcal{H}_{ETC} has the form

$$\left(\sum_{i'j'k'l'} \Lambda_{i'j'k'l'}^{q_1 q_2 \lambda_1 \lambda_2} Q_{\lambda_1 ii'}^\dagger Q_{\lambda_1 j'j} Q_{\lambda_2 kk'}^\dagger Q_{\lambda_2 l'l} \right) \bar{q}_{\lambda_1 i} \gamma^\mu q_{\lambda_1 j} \bar{q}_{\lambda_2 k} \gamma_\mu q_{\lambda_2 l}. \quad (22)$$

The Λ 's in \mathcal{H}_{ETC} are of order g_{ETC}^2/M_{ETC}^2 . A reasonable (and time-honored) guess for the magnitude of the Λ_{ijkl} is that they are comparable to the ETC coefficients that generate the quark mass matrix \mathcal{M}_q . To estimate the FCNC in \mathcal{H}_{ETC} , we elevate this to a rule: The ETC scale M_{ETC}/g_{ETC} in a term involving weak eigenstates of the form $\bar{q}'_i q'_j \bar{q}'_j q'_i$ or $\bar{q}'_i q'_i \bar{q}'_j q'_j$ (for $q'_i = u'_i$ or d'_i) is approximately the same as the scale that generates the $\bar{q}'_{Ri} q'_{Lj}$ mass term, $(\mathcal{M}_q)_{ij}$. A plausible, but approximate, scheme for correlating a quark mass $m_q(M_{ETC})$ with M_{ETC}/g_{ETC} is presented in Appendix A (see Fig. 12).

Extended technicolor masses, $M_{ETC}/g_{ETC} \gtrsim 1000 \text{ TeV}$, are necessary, but not sufficient, to suppress FCNC interactions of light quarks to an acceptable level. Without further suppression by CKM-like mixing angles, the ETC masses required for compatibility with ϵ are so large that, even with walking technicolor, light-quark masses are too small [7]. Thus, we need to assume that \mathcal{H}_{ETC} is *electroweak generation conserving*, i.e.,

$$\Lambda_{ijkl}^{q_1 q_2 \lambda_1 \lambda_2} = \delta_{il} \delta_{jk} \Lambda_{ij}^{q_1 q_2 \lambda_1 \lambda_2} + \delta_{ij} \delta_{kl} \Lambda_{ik}^{q_1 q_2 \lambda_1 \lambda_2}. \quad (23)$$

Considerable FCNC suppression then comes from off-diagonal elements in the alignment matrices $Q_{L,R}$.

Note that the TC2 and ETC interactions generally have RL $((V + A) \times (V - A))$ and RR $((V + A) \times (V + A))$ “wrong chirality” structure as well as the LL $((V - A) \times (V - A))$ and LR $((V - A) \times (V + A))$ structure found in standard model contributions to FCNC interactions.

4. Constraints on the TC2 and ETC Interactions

The first constraint we consider is that which top quark condensation, but not bottom nor light quark condensation, places on the TC2 couplings and hypercharges. In the Nambu–Jona-Lasinio approximation, a $\bar{q}q$ condensate occurs when the quark’s couplings satisfy

$$\alpha_q(V_8) + \alpha_q(Z') \equiv \frac{g_C^2 A_q^2}{3\pi^2} + \frac{g_Y^2 \cot^2 \theta_Y (Y_{Lq} Y_{Rq})}{4\pi^2} \geq 1. \quad (24)$$

The so-called critical values of the couplings occur when the equality is satisfied. As we have stressed, both terms should be $\mathcal{O}(1)$ to avoid fine tuning. In STC2, this strongly suggests that

$$Y_{Lt} Y_{Rt} > 0; \quad Y_{Lb} Y_{Rb} < 0 \quad (\text{STC2}). \quad (25)$$

Because $A_l^2 = \tan^2 \theta_C \ll 1$, the constraint on light quarks is rather loose, however:

$$g_Y^2 \cot^2 \theta_Y Y_{Lq} Y_{Rq} / 4\pi^2 < 1 \quad (\text{STC2}). \quad (26)$$

In FUTC2, the condition that only the top quark condenses is most simply met by requiring that, for all quarks except top,

$$Y_{Lq} Y_{Rq} < 0 \quad (\text{FUTC2}). \quad (27)$$

We assume this from now on.

Other limits on the couplings and masses in \mathcal{H}_{TC2} and \mathcal{H}_{ETC} come from mixing and CP violation in the K^0 and B_d meson systems. The constraint from the kaon ϵ parameter for models in which D_R is block diagonal were discussed in Refs. [20, 7]. For $\Lambda_{ssss} \simeq (2000 \text{ TeV})^{-2}$ and $M_{V_8} \simeq M_{Z'} \simeq 10 \text{ TeV}$, it was shown there it is not difficult to account for the measured value of ϵ . For models with a nontrivial D_R and these mass scales, the ϵ parameter is not a strong constraint at all. Varying the relative strengths and signs of Λ_{ssss} and Λ'_{ssss} can cause changes of up to ± 100 times the standard model ϵ . The more incisive constraint on TC2 — but not on ETC — comes from \bar{B}_d – B_d mixing. This was considered first (mainly for STC2) in Ref. [21] and reconsidered (especially for FUTC2) in Ref. [22]. We reconsider both TC2 variants in this section.

The B_H^0 – B_L^0 mass difference $\Delta M_{B_d} = (3.22 \pm 0.05) \times 10^{-10} \text{ MeV}$ is directly related to the off-diagonal matrix element M_{12} of the $\bar{B}_d - B_d$ Hamiltonian [39]. Since $|\Gamma_{12}| \ll |M_{12}|$,

we have $\Delta M_{B_d} = 2|M_{12}|$. The standard model contributions to M_{12} come from box diagrams which are proportional to V_{td}^2 and therefore carry a CKM phase -2β . New physics contributions, at tree and loop levels, can alter the magnitude and phase of M_{12} . However, M_{12} -mixing occurs in all neutral B decays, so that new physics in mixing alone *cannot* explain the $\sin 2\beta$ discrepancy (see Sect. 6).

In both FUTC2 and STC2, the dominant new contribution to M_{12} comes from $\bar{b}'b\bar{b}'b'$ terms in \mathcal{H}_{TC2} . For FUTC2, the interaction is

$$\begin{aligned} \mathcal{H}_{FU}(M_{12}) = & \frac{g_Y^2 \cot^2 \theta_Y}{8M_{Z'}^2} \left[(\Delta Y_L)^2 (D_{Lbb} D_{Lbd}^*)^2 (\bar{d}b)_{V-A} (\bar{d}b)_{V-A} \right. \\ & + (\Delta Y_R)^2 (D_{Rbb} D_{Rbd}^*)^2 (\bar{d}b)_{V+A} (\bar{d}b)_{V+A} \\ & \left. + 2(\Delta Y_L)(\Delta Y_R) (D_{Lbb} D_{Lbd}^* D_{Rbb} D_{Rbd}^*) (\bar{d}b)_{V-A} (\bar{d}b)_{V+A} + \text{h.c.} \right], \end{aligned} \quad (28)$$

where $(\bar{d}b)_{V\pm A} = \bar{d}\gamma_\mu(1\pm\gamma_5)b$ and the appearance of $\Delta Y_\lambda = Y_{\lambda b} - Y_{\lambda d}$ reflects the approximate flavor symmetry of Eq. (2). Then M_{12} is estimated in the vacuum insertion approximation to be [21, 22]:

$$\begin{aligned} 2(M_{12})_{FU} = & \frac{g_Y^2 \cot^2 \theta_Y}{3M_{Z'}^2} F_{B_d}^2 \hat{B}_{B_d} M_{B_d}^2 \eta_B \left[\Delta Y_L^2 (D_{Lbb} D_{Lbd}^*)^2 + \Delta Y_R^2 (D_{Rbb} D_{Rbd}^*)^2 \right. \\ & \left. - \left(\frac{3}{2} + \frac{M_B^2}{(m_b + m_d)^2} \right) \Delta Y_L \Delta Y_R (D_{Lbb} D_{Lbd}^* D_{Rbb} D_{Rbd}^*) \right]. \end{aligned} \quad (29)$$

For STC2 models, there is also a coloron contribution:

$$\begin{aligned} 2(M_{12})_S = & 2(M_{12})_{FU} + \frac{g_C^2 \cot^2 \theta_C}{9M_{V_8}^2} F_{B_d}^2 \hat{B}_{B_d} M_{B_d}^2 \eta_B \\ & \times \left[(D_{Lbb} D_{Lbd}^*)^2 + (D_{Rbb} D_{Rbd}^*)^2 - \left(\frac{3}{2} + \frac{M_B^2}{(m_b + m_d)^2} \right) (D_{Lbb} D_{Lbd}^* D_{Rbb} D_{Rbd}^*) \right]. \end{aligned} \quad (30)$$

Here, $\eta_B = 0.55 \pm 0.01$ is a QCD radiative correction factor for the LL and RR product of color-singlet currents and we assume it to be the same for the LR product. We take $F_{B_d} \sqrt{\hat{B}_{B_d}} = (200 \pm 40) \text{ MeV}$ [40], where F_{B_d} and B_{B_d} are, respectively, the B_d -meson decay constant and bag parameter. The additional factor of 1/3 in the coloron contribution comes from the Fierz rearrangement to a product of color singlet currents. These TC2 contributions to M_{12} are added to the standard-model one [39],

$$2(M_{12})_{SM} = \frac{G_F^2}{6\pi^2} \eta_B M_{B_d} F_{B_d}^2 M_W^2 S_0(x_t) (V_{tb}^* V_{td})^2, \quad (31)$$

where the top-quark loop function $S_0(x_t) \cong 2.3$ for $x_t = m_t^2(m_t)/M_W^2$ and $m_t(m_t) = 167 \text{ GeV}$. The TC2 contributions to M_{12} come from operators renormalized at $M_{Z'}$ and M_{V_8} rather than at M_W . For simplicity, we take $M_{Z'} = M_{V_8}$ unless stated otherwise. We assume

that operator renormalizations from $M_{Z'}$ to M_W are simply multiplicative, $\mathcal{O}(1)$, and can therefore be ignored¹⁹.

As Simmons pointed out, including the RR and LR operators in M_{12} opens the possibility of obtaining lower mass limits than in Ref. [21]. She found $M_{Z'} \gtrsim 1$ TeV in FUTC2. However, Simmons assumed smaller $U(1)_1$ couplings than we do. Furthermore, D_R and D_L matrix elements that lead to lower TC2 boson masses may not arise from alignment with plausible mass models. This, in fact, is what we found for the mass matrices considered in Appendix B.

To set the mass limits, we followed Ref. [21] in assuming that the $SU(3)_1$ and $U(1)_1$ couplings of the top quark are each half their critical value, $\alpha_t(V_8) = \alpha_t(Z') = 1/2$, i.e.,

$$g_C^2 \cot^2 \theta_C = \frac{3\pi^2}{2}, \quad g_Y^2 \cot^2 \theta_Y Y_{Lt} Y_{Rt} = 2\pi^2. \quad (32)$$

We also assumed $(\Delta Y_L)^2 \equiv (Y_{Lb} - Y_{Ld})^2 = Y_{Lt} Y_{Rt}$. These assumptions are reasonable, given the need to avoid fine-tuning, but the mass limits are somewhat sensitive to them. As noted above, we also assumed $M_{V_8} = M_{Z'}$ for STC2. Because all the mixing matrix factors are determined by the primordial quark mass matrix \mathcal{M}_q , the only remaining free parameters are the ratio of hypercharge differences, $\xi = \Delta Y_R / \Delta Y_L$, and the gauge boson masses. Equating twice the total $|M_{12}|$ to the measured ΔM_{B_d} , we determined the gauge boson mass limit as a function of ξ . The lowest possible gauge boson masses for the interval of $-5 < \xi < 5$ for STC2 and FUTC2 and the three sets of alignment matrices are:

MASS MODEL	TC2 MODEL	M_{min}	FINE TUNING
1	STC2	23.9 TeV	0.05%
2	STC2	5.0 TeV	0.9%
3	STC2	10.5 TeV	0.2%
1	FUTC2	21.3 TeV	3%
2	FUTC2	7.0 TeV	3%
3	FUTC2	10.1 TeV	3%

(33)

The last column is an estimate of the fine tuning of the TC2 couplings; this is discussed below.

In Mass Models 2 and 3, which produce $|D_{Rbq}| \simeq |D_{Lbq}|$, the bounds on $M_{V_8, Z'}$ are lower than in Model 1, as Simmons anticipated. However, this effect is not limited to FUTC2. Nor are the bounds as low as Simmons determined because she assumed a relatively weak $U(1)_1$ coupling and $Y_{Lb} Y_{Rb} = -1/18$. Although Mass Model 1 satisfies the relationship Eq. (17) used in Ref. [21], the mass limits do not agree. The disagreement is caused by using different values of V_{td} . The mass limits scale approximately as $|V_{td}|$ in Model 1. In Ref. [21], the minimal values $|V_{td}| = 0.005$ and 0.0034 were used. Here, we derived V_{td} from \mathcal{M}_q , obtaining

¹⁹Since TC2 contributions occur at tree level, Γ_{12} is unaffected. Therefore, we still have $|\Gamma_{12}| \ll |M_{12}|$, and the ratio q/p , which describes the degree of mixing in the physical eigenstates (in Eq. (53) below), is still a pure phase [39].

$|V_{td}| = .0075$ in Model 1 and $|V_{td}| = 0.0055$ in Models 2 and 3. As noted in Ref. [22], once D_R is no longer block-diagonal, the ΔM_{B_d} constraint is no longer model-independent, i.e., determined solely by the CKM element V_{td} . This is clearly demonstrated in the factor of 1.5–2 difference in the bounds for Models 2 and 3.

Finally, producing a TC2 contribution $\hat{m}_t \simeq 165$ GeV to the top quark mass with such large Z' and V_8 masses implies fine tuning of the couplings to their critical value [15]. The fine tuning is characterized by the magnitude of

$$\frac{\alpha_t(Z') \frac{\hat{m}_t^2}{M_{Z'}^2} \log \left(\frac{M_{Z'}^2}{\hat{m}_t^2} \right) + \alpha_t(V_8) \frac{\hat{m}_t^2}{M_{V_8}^2} \log \left(\frac{M_{V_8}^2}{\hat{m}_t^2} \right)}{\alpha_t(Z') \left[1 - \frac{\hat{m}_t^2}{M_{Z'}^2} \log \left(\frac{M_{Z'}^2}{\hat{m}_t^2} \right) \right] + \alpha_t(V_8) \left[1 - \frac{\hat{m}_t^2}{M_{V_8}^2} \log \left(\frac{M_{V_8}^2}{\hat{m}_t^2} \right) \right]} \quad (34)$$

In Ref. [21], with $M_{V_8} \simeq 5$ TeV and $M_{Z'} \simeq 10$ TeV, the fine tuning was found to be 0.5% using the NJL approximation with half-critical couplings. Using $M_{Z'} = M_{V_8}$ with the appropriate STC2 mass limits, we obtain the fine tuning estimates $\lesssim 1\%$ listed in Eq. (33). In FUTC2, the situation is somewhat better *if* we lower M_{V_8} to the limit allowed by precision electroweak observables, $M_{V_8} \simeq 1.6$ TeV [18]. This leads to fine tuning of 3%. Fine tuning is also ameliorated if we allow $(\Delta Y_L)^2 < Y_{Lt} Y_{Rt}$. This allows a lower $M_{Z'}$. Obviously, this difference in the hypercharges cannot be too extreme. In summary, despite more general assumptions on the structure of the alignment matrices, we find the couplings to be as fine-tuned as in Ref. [21]. The principal reason is that we insist on a large $U(1)_1$ coupling to avoid fine tuning $\alpha_t(V_8)$!

5. $B_d \rightarrow J/\psi K_S, \phi K_S, \eta' K_S$ and πK_S

With the assumption that ETC interactions are generation conserving, their contributions to B_d decays are suppressed by small mixing angles and hence negligibly small. The TC2 contributions to $b \rightarrow s \bar{q} q$ decays are obtained by writing Eqs. (20) in terms of mass eigenstates and making use of the unitarity of the $D_{L,R}$:

$$\begin{aligned} \mathcal{H}_{FU} &= \frac{g_Y^2 \cot^2 \theta_Y}{2M_{Z'}^2} \sum_{\lambda_1, \lambda_2=L,R} D_{\lambda_1 bs}^* D_{\lambda_1 bb} \Delta Y_{\lambda_1} \bar{s}_{\lambda_1} \gamma^\mu b_{\lambda_1} \sum_{j=u,d,s,c} Y_{\lambda_2 q_j} \bar{q}_{\lambda_2 j} \gamma_\mu q_{\lambda_2 j} + \text{h.c.} ; \\ \mathcal{H}_S &= \mathcal{H}_{FU} + \frac{g_C^2 \cot^2 \theta_C}{2M_{V_8}^2} \sum_{\lambda_1, \lambda_2=L,R} D_{\lambda_1 bs}^* D_{\lambda_1 bb} \bar{s}_{\lambda_1} \gamma^\mu \frac{\lambda_A}{2} b_{\lambda_1} \\ &\quad \times \left(\sum_{j=d,s} |D_{\lambda_2 bj}|^2 + \sum_{j=u,c} |U_{\lambda_2 tj}|^2 \right) \bar{q}_{\lambda_2 j} \gamma_\mu \frac{\lambda_A}{2} q_{\lambda_2 j} + \text{h.c.} . \end{aligned} \quad (35)$$

The standard model contribution to a B_d -decay interaction is written as a sum over a standard set of operators, each multiplied by the appropriate Wilson coefficient. These coefficient functions are found at M_W by calculating the necessary QCD and electroweak

(EW) penguin (loop) diagrams. We rewrite the TC2 interactions in terms of the same set of operators by Fierzing color octet products and using parity to relate matrix elements of wrong chirality operators to the standard ones. The TC2 coefficient functions involve combinations of hypercharges and $U(1)_1$ and $SU(3)_1$ couplings rather than loop factors.

The standard operators have LL and LR chirality. Casting the RR and RL operators from TC2 in the same color and charge structure as these, we obtain the eight wrong chirality operators

$$\begin{aligned}
\hat{Q}'_3 &= (\bar{s}b)_{V+A} \sum_q (\bar{q}q)_{V+A} & \hat{Q}'_5 &= (\bar{s}b)_{V+A} \sum_q (\bar{q}q)_{V-A} \\
\hat{Q}'_4 &= (\bar{s}_\alpha b_\beta)_{V+A} \sum_q (\bar{q}_\beta q_\alpha)_{V+A} & \hat{Q}'_5 &= (\bar{s}_\alpha b_\beta)_{V+A} \sum_q (\bar{q}_\beta q_\alpha)_{V-A} \\
\hat{Q}'_7 &= \frac{3}{2}(\bar{s}b)_{V+A} \sum_q e_q (\bar{q}q)_{V-A} & \hat{Q}'_9 &= \frac{3}{2}(\bar{s}b)_{V+A} \sum_q e_q (\bar{q}q)_{V+A} \\
\hat{Q}'_8 &= \frac{3}{2}(\bar{s}_\alpha b_\beta)_{V-A} \sum_q e_q (\bar{q}_\beta q_\alpha)_{V+A} & \hat{Q}'_{10} &= \frac{3}{2}(\bar{s}_\alpha b_\beta)_{V+A} \sum_q e_q (\bar{q}_\beta q_\alpha)_{V+A}, \quad (36)
\end{aligned}$$

where e_q is the charge of quark q . The total TC2 contribution is the sum of the standard and wrong chirality portions.²⁰

$$\mathcal{H}_{eff,TC2}(\mu = M_{Z'}) = \frac{G_F}{\sqrt{2}} \sum_{i=3}^{10} \left(C_{i,TC2}(\mu) \hat{Q}_i(\mu) + C'_{i,TC2}(\mu) \hat{Q}'_i(\mu) \right). \quad (37)$$

Using parity For B_d -decays to a pair of pseudoscalars or a pseudoscalar and a vector,

$$\langle PP | \hat{Q}'_i | B_d \rangle = -\langle PP | \hat{Q}_i | B_d \rangle, \quad \langle PV | \hat{Q}'_i | B_d \rangle = +\langle PV | \hat{Q}_i | B_d \rangle. \quad (38)$$

the effective Hamiltonian reduces to a sum over standard operators alone:

$$\mathcal{H}_{eff,TC2} = \frac{G_F}{\sqrt{2}} \sum_{i=3}^{10} (C_{i,TC2} \pm C'_{i,TC2}) \hat{Q}_i, \quad (39)$$

where the $+$ ($-$) sign is for $B_d \rightarrow PV$ (PP).

The Wilson coefficient contributions $\tilde{C}_i = C_i \pm C'_i$ from coloron and Z' interactions are tabulated below. They are to be multiplied by the mixing factor $D_{Lbb} D_{Lbs}^* \simeq V_{tb} V_{ts}^*$ and by

²⁰A factor of $G_F/\sqrt{2}$ has been taken out for easy comparison with the standard model contribution.

$\sqrt{2}/(4G_F)$. The coloron contributions are (up to smaller terms of $\mathcal{O}(|D_{Lbd}|^2)$):

$$\begin{aligned}
\tilde{C}_{3,V_8} &= -\frac{g_C^2 \cot^2 \theta_C}{2M_C^2} \frac{|D_{Lbs}|^2}{9} (1 \pm \chi^3 e^{i\delta}) \\
\tilde{C}_{4,V_8} &= \frac{g_C^2 \cot^2 \theta_C}{2M_C^2} \frac{|D_{Lbs}|^2}{3} (1 \pm \chi^3 e^{i\delta}) \\
\tilde{C}_{5,V_8} &= -\frac{g_C^2 \cot^2 \theta_C}{2M_C^2} \frac{|D_{Lbs}|^2}{9} (\chi^2 \pm \chi e^{i\delta}) \\
\tilde{C}_{6,V_8} &= \frac{g_C^2 \cot^2 \theta_C}{2M_C^2} \frac{|D_{Lbs}|^2}{3} (\chi^2 \pm \chi e^{i\delta}) \\
\tilde{C}_{7,V_8} &= \frac{g_C^2 \cot^2 \theta_C}{2M_C^2} \frac{|D_{Lbs}|^2}{9} (\chi^2 \pm \chi e^{i\delta}) \\
\tilde{C}_{8,V_8} &= -\frac{g_C^2 \cot^2 \theta_C}{2M_C^2} \frac{|D_{Lbs}|^2}{3} (\chi^2 \pm \chi e^{i\delta}) \\
\tilde{C}_{9,V_8} &= \frac{g_C^2 \cot^2 \theta_C}{2M_C^2} \frac{|D_{Lbs}|^2}{9} (1 \pm \chi^3 e^{i\delta}) \\
\tilde{C}_{10,V_8} &= -\frac{g_C^2 \cot^2 \theta_C}{2M_C^2} \frac{|D_{Lbs}|^2}{3} (1 \pm \chi^3 e^{i\delta})
\end{aligned} \tag{40}$$

The Z' contributions are:

$$\begin{aligned}
\tilde{C}_{3,Z'} &= \frac{g_Y^2 \cot^2 \theta_Y (\Delta Y_L)^2}{2M_{Z'}^2} \left(\frac{Y_{Ld}}{\Delta Y_L} \pm \frac{2Y_{Rd} + Y_{Ru}}{3\Delta Y_L} \xi \chi e^{i\delta} \right) \\
\tilde{C}_{5,Z'} &= \frac{g_Y^2 \cot^2 \theta_Y (\Delta Y_L)^2}{2M_{Z'}^2} \left(\frac{2Y_{Rd} + Y_{Ru}}{3\Delta Y_L} \pm \frac{Y_{Ld}}{\Delta Y_L} \xi \chi e^{i\delta} \right) \\
\tilde{C}_{7,Z'} &= \frac{g_Y^2 \cot^2 \theta_Y (\Delta Y_L)^2}{2M_{Z'}^2} \left(\frac{2(Y_{Ru} - Y_{Rd})}{3\Delta Y_L} \right) \\
\tilde{C}_{9,Z'} &= \frac{g_Y^2 \cot^2 \theta_Y (\Delta Y_L)^2}{2M_{Z'}^2} \left(\pm \frac{2(Y_{Ru} - Y_{Rd})}{3\Delta Y_L} \xi \chi e^{i\delta} \right)
\end{aligned} \tag{41}$$

The free parameters are ξ , χ , and δ , defined by

$$\xi = \frac{\Delta Y_R}{\Delta Y_L}, \quad \chi = \left| \frac{D_{Rbs}}{D_{Lbs}} \right|, \quad \delta = \arg \left(\frac{D_{Rbb} D_{Rbs}^*}{D_{Lbb} D_{Lbs}^*} \right). \tag{42}$$

The V_8 and Z' coefficients appear in the effective STC2 Hamiltonian, while in FUTC2, the coloron coefficients are absent. The gluonic and electroweak color singlet penguin operators $\hat{Q}_3, \hat{Q}_5, \hat{Q}_7$, and \hat{Q}_9 receive contributions from both coloron and Z' exchange, while the color octet product penguin operators $\hat{Q}_4, \hat{Q}_6, \hat{Q}_8$, and \hat{Q}_{10} receive only coloron contributions. There is no TC2 contribution to the standard tree level operators \hat{Q}_1, \hat{Q}_2 . In the definitions of $\tilde{C}_{i,TC2}$, we imposed the hypercharge restrictions in Eq. (2). The nonstandard CP-violating terms are proportional to D_{Rbs}/D_{Lbs} . For models with D_R nearly block-diagonal, the TC2 contributions are therefore coherent with the standard ones and do not cause a $\sin 2\beta$ discrepancy.

We have neglected the standard model contributions from penguin operators with internal up or charm quarks. These contain CP conserving phases and are consequently the source of direct CP violation within the standard model. Since the TC2 interactions we have included are all tree level interactions, the total SM + TC2 Hamiltonian will contain no direct CP violation. For simplicity we have also neglected standard electromagnetic penguin and chromomagnetic penguin operators. For reviews that include these operators and their possible influence on CP violating B decays see Ref.[41, 42]

To combine TC2 and standard-model effects, we need to run the TC2 contributions from $M_{Z'}$ down to M_W using the renormalization group equation (RGE). The RGE for the coefficient functions of the standard $\Delta B = 1$ operators is known and has been calculated to several orders in α_s (see Ref. [43]). Loop-level gluon ($SU(3)_{1,2}$ gauge boson) effects can mix the operators, so the RGE for the coefficient functions is a matrix equation.

An important approximation we make to obtain the RGE is to consider only QCD renormalization effects. Electroweak contributions are negligible. But strong $U(1)_1$ and $SU(3)_1$ (in FUTC2) renormalizations are not. The former are very model-dependent and their effect hard to predict. The latter are intractable because of the strong $\alpha_C \cot \theta_C$ coupling, but it is not implausible that they do not alter the pattern of operator mixing. The RGE is then

$$C_{i,TC2}(M_W) = \sum_j \hat{U}(M_{Z'}, M_W)_{ij} C_{j,TC2}(M_{Z'}),$$

$$\hat{U}(M_{Z'}, M_W)_{ij} = \exp \left[\int_{g_1(M_W)}^{g_1(M_{Z'})} dx \frac{\gamma^T(x)_{ij}}{\beta(x)} \right]. \quad (43)$$

Here $\gamma^T(x)$ is the transposed anomalous dimension matrix, and $\beta(x)$ the QCD beta function. In our calculations, we used the $\mathcal{O}(\alpha_C)$ β and γ -functions [43] and included only standard model particles²¹. After running the TC2 effects, we have the total standard plus TC2 Hamiltonian at M_W .

$$\mathcal{H}_{\text{eff}}(M_W) = \frac{G_F}{\sqrt{2}} \left[V_{ub}V_{us}^* (C_1 \hat{Q}_1^u + C_2 \hat{Q}_2^u) + V_{cb}V_{cs}^* (C_1 \hat{Q}_1^c + C_2 \hat{Q}_2^c) - V_{tb}V_{ts}^* \sum_{i=3}^{10} (C_{i,SM} - \tilde{C}_{i,TC2}) \hat{Q}_i \right]. \quad (44)$$

Finally, we run the standard-model plus TC2 Wilson coefficients from M_W down to the desired energy μ (here, m_b):

$$C_i(\mu) = \sum_j \hat{U}(M_W, \mu)_{ij} C_j(M_W), \quad (45)$$

where

$$C_i(M_W) = C_{i,SM}(M_W) + \sum_j \hat{U}(M_{Z'}, M_W)_{ij} C_{j,TC2}(M_{Z'}). \quad (46)$$

²¹We adjusted the renormalization and subtraction scheme in [43] to be consistent with the current results for M_W , m_t , and α_s

The evolution matrix in $C_i(\mu)$ has the same form as in Eq. (43) except that limits involve the QCD coupling g_C rather than the $SU(3)_1$ coupling. The anomalous dimension matrix and the beta function in Eq. (45) include only five quark flavors. The resulting Hamiltonian, with possible new CP-violating phases from D_R , is

$$\mathcal{H}_{\text{eff}}(b \rightarrow s\bar{q}q) = \frac{G_F}{\sqrt{2}} V_{tb}V_{ts}^* \sum_i \tilde{D}_i(\mu) \hat{Q}_i(\mu) \quad (47)$$

where

$$\tilde{D}_i(\mu) = \sum_j \hat{U}(M_W, \mu)_{ij} \left(C_{j,SM}(M_W) + \sum_k \hat{U}(M_{Z'}, M_W)_{jk} C_{k,TC2}(M_{Z'}) \right). \quad (48)$$

To apply this Hamiltonian to a particular $b \rightarrow s\bar{q}q$ process, we evaluate the amplitude using the factorization approximation [44, 45]. There the operators are split into two sub-currents:

$$\langle h_1 h_2 | \hat{Q}_i = j_{1\mu} j_{2\mu}^\dagger | B_d \rangle \cong \langle h_1 | j_{1\mu} | 0 \rangle \langle h_2 | j_{2\mu}^\dagger | B_d \rangle + \langle h_2 | j_{1\mu} | 0 \rangle \langle h_1 | j_{2\mu}^\dagger | B_d \rangle, \quad (49)$$

where we ignored annihilation terms such as $\langle h_1 h_2 | j_{1\mu} | 0 \rangle \langle 0 | j_{2\mu} | B \rangle$. The $\langle h_i | j_\mu | B_d \rangle$ portion is a form factor that can be measured in a semileptonic decay, while $\langle h_j | j_\mu | 0 \rangle$ is a measurable decay constant. The values of the form factors and decay constants we used in our calculations can be found in Ref. [44]. Different operators with different chiral and color prefactors will contribute depending on the particular decay process. For example:

$$\begin{aligned} A(B \rightarrow \phi K_S) \propto & \langle \phi | (\bar{s}s)_{V-A} | 0 \rangle \langle K_S | (\bar{s}b)_{V-A} | B \rangle \left[(\tilde{D}_3 + \tilde{D}_4 - \frac{1}{2}\tilde{D}_9 - \frac{1}{2}\tilde{D}_{10}) \left(\frac{1}{N_{QCD}} + 1 \right) \right. \\ & \left. + \tilde{D}_5 - \frac{1}{2}\tilde{D}_7 + \frac{1}{N_{QCD}}(\tilde{D}_6 - \frac{1}{2}\tilde{D}_8) \right]. \end{aligned} \quad (50)$$

The factorized amplitude includes only the contribution from color singlet operators. To compensate for the contributions from other operators, the number of color N_C is treated as a parameter²². Because of the possible dependency on the effective number of colors (and other more technical reasons), we caution that the factorization approximation is not a good approximation for all modes. Factorization for the decay modes $\eta' K_S, \pi K_S$, and to some extent ϕK_S , is considered to be reliable [45].²³ After the amplitude is factored, it is useful to separate its real and imaginary parts:

$$\begin{aligned} A(B \rightarrow f) &= V_{CKM}(\mathcal{X} + i\mathcal{Y}), \\ \mathcal{X} &= \sum_i \text{Re}(a_i \tilde{D}_i), \quad \mathcal{Y} = \sum_i \text{Im}(a_i \tilde{D}_i). \end{aligned} \quad (51)$$

where the a_i are numerical factors multiplying the coefficient functions (\tilde{D}_i) in the factorized amplitude and V_{CKM} is the standard model CKM factor for the process. *In models with block-diagonal D_R , $\mathcal{Y} \cong 0$ for the $B_d \rightarrow X K_S$ decays we consider and all correct measurements return the same value of $\sin 2\beta$.*

²²For all calculations we use $N_C = 3$

²³Due to tree dominance of the J/ψ mode, factorization is not carried out in the same manner as the other modes, but it is still reliable.

6. The extraction of $\sin 2\beta_{\text{eff}}$

With the Hamiltonian in Eq. (47) renormalized and factorized at m_b , we proceed with the standard CP formalism described in many review papers [39, 46]. The asymmetry we are interested in for comparison to $\sin 2\beta$ involves interference between the \bar{B}_d - B_d mixing phase ϕ_M and the decay phase ϕ_D . It is defined by

$$a_{MD}(t) = \frac{\Gamma(B_{phys}^0(t) \rightarrow f) - \Gamma(\bar{B}_{phys}^0(t) \rightarrow f)}{\Gamma(B_{phys}^0(t) \rightarrow f) + \Gamma(\bar{B}_{phys}^0(t) \rightarrow f)}. \quad (52)$$

The state B_{phys}^0 is a meson that started at production time $t = 0$ as a B_d but contains both B_d and \bar{B}_d at later times. The CP asymmetry is described in terms of the phase-convention-independent parameter λ_{CP} :

$$\lambda_{CP} = \left(\frac{q}{p}\right) \frac{A(\bar{B}^0 \rightarrow \bar{f})}{A(B^0 \rightarrow f)} = \eta \left(\frac{q}{p}\right) \frac{A(\bar{B}^0 \rightarrow f)}{A(B^0 \rightarrow f)} \quad (53)$$

where η is the CP eigenvalue of the final state.²⁴ The q/p factor comes from B mixing and describes the proportion of B_d to \bar{B}_d in the mass eigenstates. It is a pure phase, but with the addition of TC2 effects that phase may no longer be $\beta = \arg(V_{td}^*)$, so we write

$$\left(\frac{q}{p}\right)_{TC2} = e^{-2i\phi_M}. \quad (54)$$

We can write Eqs. (29,30) as the standard model phase $\arg(2V_{td}^*)$ times some complex number. The phase of this complex number is the nonstandard mixing phase. Since only the TC2_{LR} and TC2_{RR} contributions contain phases different from $\arg(2V_{td}^*)$, the mixing phase is

$$\phi_M = \arg(V_{td}^*) + \arctan \left[\frac{\text{Im}(\text{TC2}_{RR} + \text{TC2}_{LR})}{\text{Re}(\text{SM} + \text{TC2})} \right]. \quad (55)$$

In the standard model, the amplitude ratio \bar{A}/A for the decay modes $B_d \rightarrow XK_S$ has unit magnitude and no imaginary part (to within 4%).

Since our standard plus TC2 Hamiltonian contains no sources of direct CP violation, the magnitude of the amplitude ratio will not change. The addition of TC2 effects therefore alters only the phase of \bar{A}/A :

$$\phi_D = \frac{1}{2} \arctan \left[\frac{-2\mathcal{X}\mathcal{Y}}{\mathcal{X}^2 - \mathcal{Y}^2} \right], \quad (56)$$

and \mathcal{X} and \mathcal{Y} are the real and imaginary parts of A (see Eq. (51)). It is possible to obtain a $\sin 2\beta$ discrepancy with an additional decay phase but no additional mixing phase. The value of ϕ_D depends on the final state, since the operators that contribute to a decay and their relative strength depend on the decay mode and are determined by the factorization. If there is no new CP-violating decay phase, then $\mathcal{Y} = \phi_D = 0$.

²⁴Therefore this formalism only applies to final states that are CP eigenstates.

Expressed in terms of λ_{CP} , the asymmetry at time t is

$$a_{MD} = \frac{(1 - |\lambda_{CP}|^2) \cos(\Delta Mt) - 2\text{Im}(\lambda_{CP}) \sin(\Delta Mt)}{(1 + |\lambda_{CP}|^2)} \quad (57)$$

The term we are interested in is the one proportional to $\text{Im}(\lambda_{CP})$. In the standard model, $\phi_D = 0$ so that $\text{Im}(\lambda_{CP}) = -\sin 2\beta$. In TC2 models, the $\text{Im}(\lambda_{CP})$ term becomes

$$\sin 2\beta_{\text{eff}} = \sin(2(\phi_M - \phi_D)). \quad (58)$$

Any discrepancy among the various decay modes is therefore due to differing decay phases.

7. Comparisons with Experiment

7.1 $\sin 2\beta_{\text{eff}}$ in $B_d \rightarrow XK_S$ Decays

Using this formalism, we calculated $\sin 2\beta_{\text{eff}}$ for the decays $B_d \rightarrow J/\psi K_S$, ϕK_S , $\eta' K_S$ and πK_S . The current experimental values are recorded again here. They are unsettled, but seem to show a discrepancy, especially between $J/\psi K_S$ and the Belle measurement of ϕK_S and, possibly, $\eta' K_S$:

$$\begin{aligned} \sin 2\beta_{J/\psi K_S} &= +0.72 \pm 0.05 & [1] \\ \sin 2\beta_{\phi K_S} &= +0.47 \pm 0.34 & (\text{Babar } [2]) \\ \sin 2\beta_{\phi K_S} &= +0.06 \pm 0.33 & (\text{Belle } [3]) \\ \sin 2\beta_{\eta' K_S} &= +0.27 \pm 0.21 & [4] \\ \sin 2\beta_{\pi K_S} &= +0.48^{+0.38}_{-0.47} \pm 0.11 & [5] \end{aligned} \quad (59)$$

In Mass Model 1, $|D_{Rbs}| \ll |D_{Lbs}|$ and $|D_{Rbd}| \ll |D_{Lbd}|$, so $\sin 2\beta_{\text{eff}}$ is the same for all modes, with $\beta_{\text{eff}} = \arg(V_{td}^*) = 0.516$ (see Appendix B). This and the other models were not tuned to give $\arg(V_{td}^*) = \beta_{J/\psi K_S}$, but it would not be difficult to do so. Nor did we attempt to match the experimental $V_{cb} \simeq 0.04$, so that the $|V_{ts}| \simeq |V_{cb}|$ we use below to determine the standard model's contribution to ΔM_{B_s} is too small.

There can be a sizable differences in the values of $\sin 2\beta_{\text{eff}}$ for $J/\psi K_S$ and the other modes in Mass Model 2. The discrepancies $|\sin 2\beta_{XK_S} - \sin 2\beta_{J/\psi K_S}|$ are plotted in Figs. 1–6 for both TC2 variants as a function of the parameters Y_{Ru} and Y_{Rd} .²⁵ We again assumed the Z' and V_8 couplings are half-critical (Eq. (32)) and that $\Delta Y_L^2 = Y_{Lt} Y_{Rt}$. To maximize the TC2 contribution, we used the lowest bounds on $M_{Z'} = M_{V_8}$ found in Eq. (33). (For a similar analysis that contains only the coloron contribution, see Ref. [23]). The parameters $\Delta Y_L = -0.5$ and $Y_{Lq} = 1$ were chosen to avoid light quark condensation. Only negative hypercharges, Y_{Ru} and Y_{Rd} , are included in the FUTC2 variant because of condensation

²⁵The sharp features in these figures are caused by the arctangent in the expression for ϕ_D becoming large whenever the argument in the denominator of (56) approaches zero.

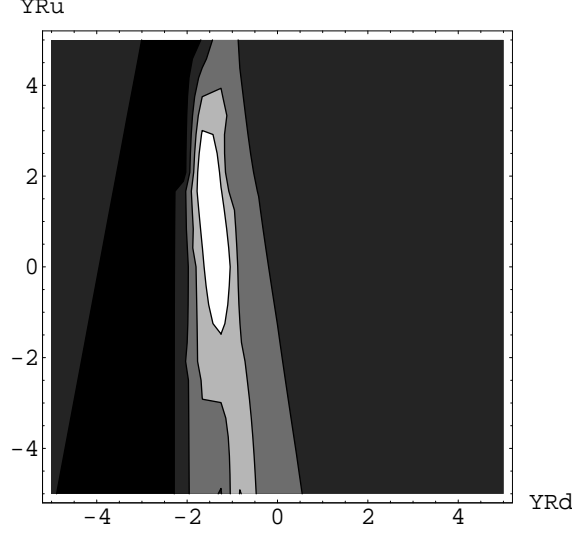


Figure 1: Discrepancy $|\sin 2\beta_{\phi K_S} - \sin 2\beta_{J/\psi K_S}|$ in the STC2 variant of Mass Model 2 as a function of Y_{Rd} and Y_{Ru} . $|\sin 2\beta_{\phi K_S} - \sin 2\beta_{J/\psi K_S}| \geq 1$ (black), > 0.75 , > 0.5 , > 0.25 , < 0.25 (white).

constraints. Clearly, large discrepancies are possible in both TC2 variants. In STC2, $|Y_{Ru}|$ and $|Y_{Rd}| \lesssim 2$ are sufficient to produce the central values of the discrepancies. Because of the larger M_{Z', V_8} in FUTC2, somewhat larger $|Y_{Rd}|$ are needed to produce the discrepancies for ϕK_S and $\eta' K_S$. As we have discussed, large hypercharges and a strong $U(1)_1$ coupling are problematic because they make the $U(1)_1$ Landau pole occur at an uncomfortably low scale.

In Mass Model 3, the only appreciable difference from $\sin 2\beta_{\text{eff}}$ for $J/\psi K_S$ for moderate hypercharges occurs for ϕK_S in the STC2 variant of the model. This case is shown in Fig. 7. Large discrepancies in the FUTC2 case require even larger hypercharges than in Model 2. The discrepancies are generally much smaller than in Model 2 because M_{Z', V_8} are about twice as large in Model 3.

7.2 Other TC2 Effects: ΔM_{B_s} and ϵ'/ϵ

With M_{Z', V_8} and $\Delta Y_R/\Delta Y_L$ deduced from ΔM_{B_d} , we can predict ΔM_{B_s} . Its experimental lower bound is $8.622 \times 10^{-9} \text{ MeV}$ [34]. The formalism for calculating the mass difference is similar to that used to obtain Eqs. (29,30) for $M_{12}(B_d)$. As before, ETC contributions are negligible because we assumed they are generation-conserving up to mass mixing. For TC2, the strange quark mass m_s replaces m_d , the CKM factor changes to $V_{tb}V_{ts}^*$, and $D_{L,Rbd}^*$ to $D_{L,Rbs}^*$. Additionally, the $SU(3)$ -breaking difference between $F_{B_s}\sqrt{\hat{B}_s}$ and $F_{B_d}\sqrt{\hat{B}_d}$ is included. As was the case for ΔM_{B_d} , all TC2 contributions occur at tree level, leaving

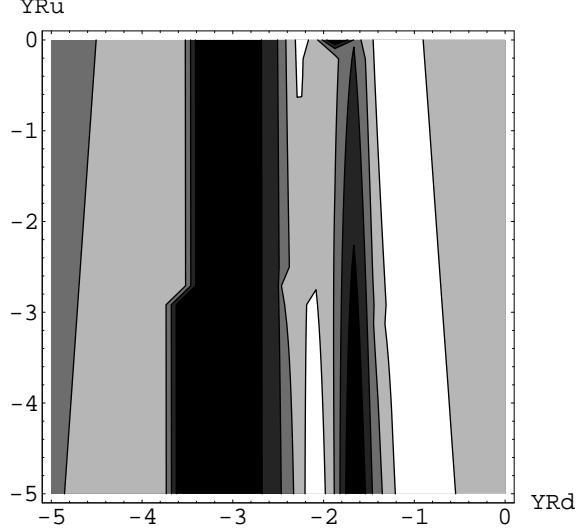


Figure 2: Discrepancy $|\sin 2\beta_{\phi K_S} - \sin 2\beta_{J/\psi K_S}|$ in the FUTC2 variant of Model 2, as a function of Y_{Rd} and Y_{Ru} . Greyscale is the same as in Fig. 1.

$\Gamma_{12}(B_s)$ unchanged from its standard model prediction.

The mass difference ΔM_{B_s} was calculated in both TC2 variants of Mass Models 1–3, using the TC2 gauge boson masses in Eq. (33). We obtained for ΔM_{B_s} and $x_s = \Delta M_{B_s}/\Gamma_{B_s}$:

<u>MASS MODEL</u>	<u>TC2 MODEL</u>	<u>$\Delta M_{B_s}(\text{MeV}) \times 10^{-8}$</u>	<u>x_s</u>
1	STC2	1.24	27
2	STC2	13.2	293
3	STC2	1.03	23
(60)			
1	FUTC2	1.24	27
2	FUTC2	3.99	88
3	FUTC2	1.01	22

The agreement between the two cases in Model 1 is fortuitous. The values would be different had we used values of $M_{V_8} = M_{Z'}$ larger than the lower bounds. The standard model contribution to ΔM_{B_s} is 8.96×10^{-9} MeV, slightly larger than the current experimental lower bound. The results for Mass Model 2 are quite different. The standard model contribution is smaller in this case, $(\Delta M_{B_s})_{SM} = 4.48 \times 10^{-9}$ MeV, because $|V_{ts}| \cong |D_{Lbs} D_{Lbb}^*|$ is smaller than it is in Model 1. Had we tuned our CKM matrix to give the value of $|V_{ts}| \cong |V_{cb}|$ in Ref. [34], it would double. The TC2 contribution is much larger here than that from the standard model because M_{Z', V_8} are 20–30% what they are in Model 1. The smaller values of ΔM_{B_s} in Model 3 are due mainly to the larger TC2 boson masses. The standard model contribution in this case is the same as in Model 2 since Models 2 and 3 have almost identical CKM matrices. For

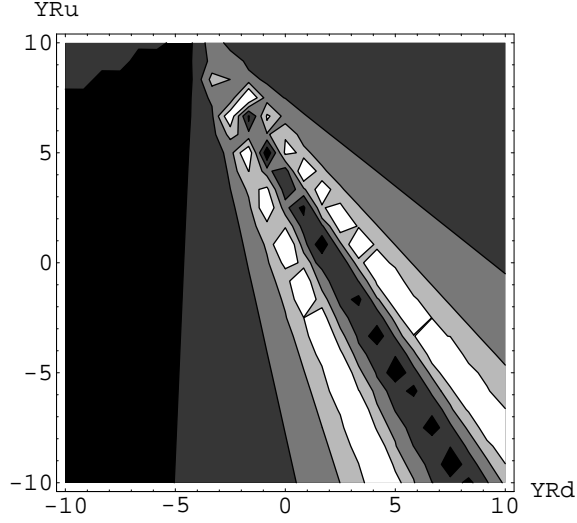


Figure 3: $|\sin 2\beta_{\eta'K_S} - \sin 2\beta_{J/\psi K_S}|$ as a function of Y_{Rd} and Y_{Ru} in the STC2 variant of Model 2. Greyscale is the same as in Fig. 1.

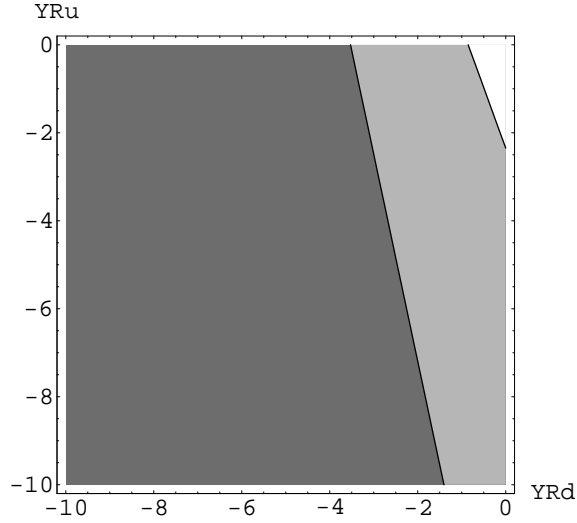


Figure 4: $|\sin 2\beta_{\eta'K_S} - \sin 2\beta_{J/\psi K_S}|$ as a function of Y_{Rd} and Y_{Ru} in the FUTC2 variant of Model 2. Greyscale is the same as in Fig. 1.

all of these mass models, TC2 contributions have a much larger effect on ΔM_{B_s} than they do on ΔM_{B_d} because the CKM factor is larger: $|V_{tb}V_{ts}^*| \cong |D_{Lbb}D_{Lbs}^*| \sim 5|V_{tb}V_{td}^*| \cong 5|D_{Lbb}D_{Lbd}^*|$. In short, our TC2 mass models can accommodate values of x_s ranging from 1 to 15 times the current experimental lower bound.

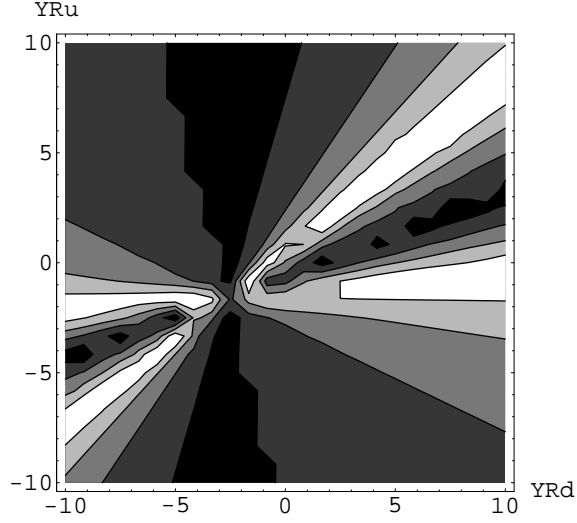


Figure 5: $|\sin 2\beta_{\pi K_S} - \sin 2\beta_{J/\psi K_S}|$ as a function of Y_{Rd} and Y_{Ru} in the STC2 variant of Model 2. Greyscale is the same as in Fig. 1.

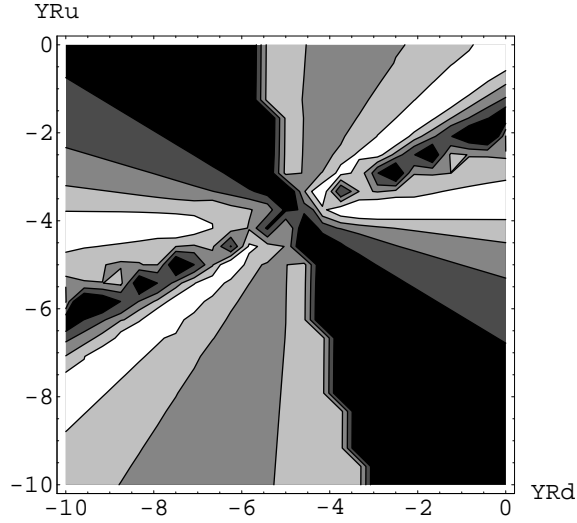


Figure 6: $|\sin 2\beta_{\pi K_S} - \sin 2\beta_{J/\psi K_S}|$ as a function of Y_{Rd} and Y_{Ru} in the FUTC2 variant of Model 2. Greyscale is the same as in Fig. 1.

Finally, we calculated the quantity $\text{Re}(\epsilon'/\epsilon)$ measuring the ratio of direct to indirect CP violation in $K^0 \rightarrow \pi\pi$ decays. It depends on the relative size and phases of the $\Delta I = \frac{3}{2}$ and $\Delta I = \frac{1}{2}$ amplitudes. Tree level and EW penguin operators contribute to both isospin portions, while gluonic penguin operators contribute only to $\Delta I = \frac{1}{2}$. The world-average

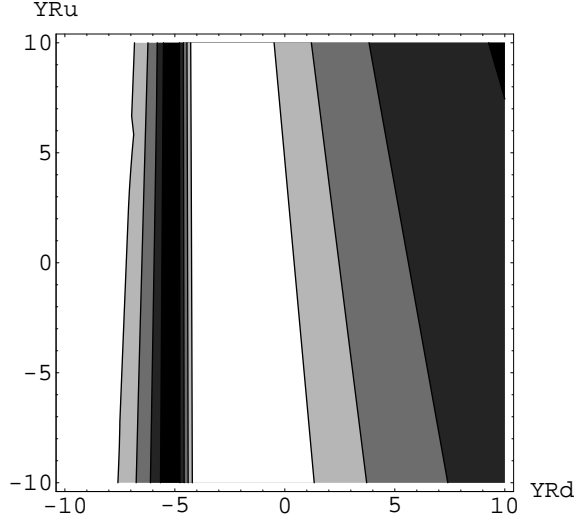


Figure 7: $|\sin 2\beta_{\phi_{K_S}} - \sin 2\beta_{J/\psi K_S}|$ as a function of Y_{Rd} and Y_{Ru} in the STC2 variant of Mass Model 3. Greyscale is the same as in Fig. 1.

experimental value is $\text{Re}(\epsilon'/\epsilon) = 16.6 \pm 1.6 \times 10^{-4}$ [47] while the latest standard model predictions are in the range $5\text{--}30 \times 10^{-4}$ [48].

The TC2 contributions to $K^0 \rightarrow \pi\pi$ are incorporated following the procedure of Sect. 5.²⁶ They are written in terms of standard $\Delta S = 1$ operators, run down to M_W using the RGE, and combined with the standard model contributions. The TC2 $\Delta S = 1$ Wilson coefficients before running are similar to the $\Delta B = 1$ coefficients in Eqs. (40,41), with m_s replacing m_b , and $D_{\lambda bs} D_{\lambda bd}^*$ replacing $D_{\lambda bb} D_{\lambda bd}^*$. For this kaon system observable, the standard model plus TC2 Hamiltonian must be evaluated near 1 GeV. Running down to m_b is carried out in the same way as before. To evolve from m_b to 1 GeV, we must remove the bottom and charm quarks at the appropriate energies. This requires successively mapping a five quark theory onto an effective four quark theory, then the four quark theory onto a three quark one; see Ref. [43].

Once the effective Hamiltonian at 1 GeV is obtained, the expression for $\text{Re}(\epsilon'/\epsilon)$ including TC2 contributions can be obtained by generalizing the expressions given in (see Refs. [43, 47])

$$\text{Re}\left(\frac{\epsilon'}{\epsilon}\right) = \text{Im}\left[V_{ts} V_{td}^* (P_{tot}^{(1/2)} - P_{tot}^{(3/2)})\right]. \quad (61)$$

Here, $P_{tot}^{(\Delta I)}$ contains the matrix elements of the standard model plus the $|\Delta I| = \frac{1}{2}$ and $\frac{3}{2}$

²⁶The ETC contributions to $K^0 \rightarrow \pi\pi$, calculated at the ETC scale, are highly suppressed by the large ETC gauge boson masses and by mixing angles. (They were first estimated in 2000 by G. Burdman (unpublished), and we concur with him.) Running effects may enhance them, but not enough to make them comparable to the standard model contributions — except, possibly, in the case of FUTC2 where quarks have strong $SU(3)_1$ interactions. As for Eq. (11), we assume that quark anomalous dimensions are not large in FUTC2.

contributions from TC2.²⁷ The additional phases in the TC2 contributions may make these matrix elements complex. We use as inputs the experimental values $\epsilon = (2.271 \pm 0.017) \times 10^{-3} \exp(i\pi/4)$, the $\Delta I = \frac{1}{2}$ amplitude $\text{Re}A_0 = 3.33 \times 10^{-7} \text{ GeV}$, and the ratio $\text{Re}A_2/\text{Re}A_0 = 0.045$. Only ϵ receives appreciable ETC and TC2 contributions and, as we noted earlier, it is not a stringent constraint on TC2. The other two inputs ($\text{Re}A_0$ and $\text{Re}A_2/\text{Re}A_0$) have mainly standard model contributions. Using the same values for ΔY_L and Y_{Ld} as for $\sin 2\beta$, we calculated $\text{Re}(\epsilon'/\epsilon)$ as a function of the Y_{Rd} and Y_{Ru} hypercharges. In the table in Eq. (62), we list the standard model contribution — whose phase is contained in $\text{Im}(V_{ts}V_{td}^*)$, the TC2 contribution involving Y_{Ld} — whose phase is the same, and the TC2 contribution from D_R , which is proportional to $Y_{Rd} - Y_{Ru}$, i.e., $\text{Re}(\epsilon'/\epsilon) = \text{SM} + \text{TC2}(Y_{Ld}) + \text{TC2} \times (Y_{Rd} - Y_{Ru})$. The V_8 contribution is negligible compared to the standard one.

<u>MASS MODEL</u>	<u>TC2 MODEL</u>	<u>SM $\times 10^{-4}$</u>	<u>TC2(Y_{Ld}) $\times 10^{-4}$</u>	<u>TC2 $\times (Y_{Rd} - Y_{Ru})10^{-4}$</u>
1	STC2	13.3	-0.18	27
2	STC2	10.3	-10.8	422
3	STC2	10.1	-0.50	100
1	FUTC2	13.3	-0.23	34
2	FUTC2	10.3	-5.52	217
3	FUTC2	10.1	-0.53	107

(62)

In Figs. 8–10 we plot, for the Models 1 and 2, bands in the Y_{Rd} – Y_{Ru} plan corresponding to two and five sigma spreads from the central experimental value of $\text{Re}(\epsilon'/\epsilon)$. For Models 1 and 3 the plots of $\text{Re}(\epsilon'/\epsilon)$ in FUTC2 and in STC2 are nearly identical, a result of both TC2 variants having approximately the same minimum Z' mass. It is clear from the table that $Y_{Rd} - Y_{Ru}$ must be close to zero (very close for Model 2) and slightly negative. The two hypercharges must be so close in Model 2 that they would be a strain on building a complete model with its mass matrix.

Summary

We have reviewed how vacuum alignment in technicolor theories causes spontaneous CP violation, and we described a possible natural solution to the quarks' strong CP problem — one which has *no axion* and *no massless up quark*. In these theories, flavor mixing and CP violation appears in the standard weak interactions, as well as in new four-fermion ETC and TC2 interactions. We explored the compatibility of these new effects with current measurements, especially of $\sin 2\beta_{\text{eff}}$. In contrast with previous work [7, 21], we did not limit ourselves to alignment models with mixing and CP violation solely in the left handed quark sector, i.e., in the D_L alignment matrix.

²⁷The $|\Delta I| = \frac{1}{2}$ and $\frac{3}{2}$ matrix elements were taken from Ref. [43, 47], except for $\langle \hat{Q}_6 \rangle_0$ and $\langle \hat{Q}_8 \rangle_2$, where we used the large- N_C lattice results given in Ref. [39].

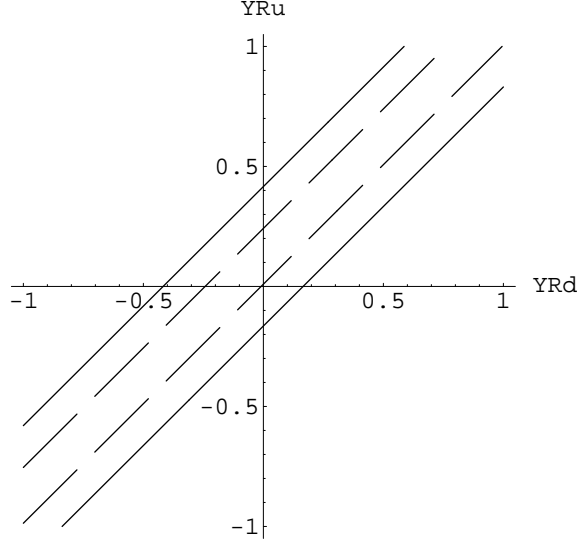


Figure 8: $\text{Re}(\epsilon'/\epsilon)$ as a function of Y_{Rd} and Y_{Ru} in the STC2 variant of Model 1. Solid lines indicate $\pm 5\sigma$, dashed lines $\pm 2\sigma$ from the central experimental value of 16.6×10^{-4} .

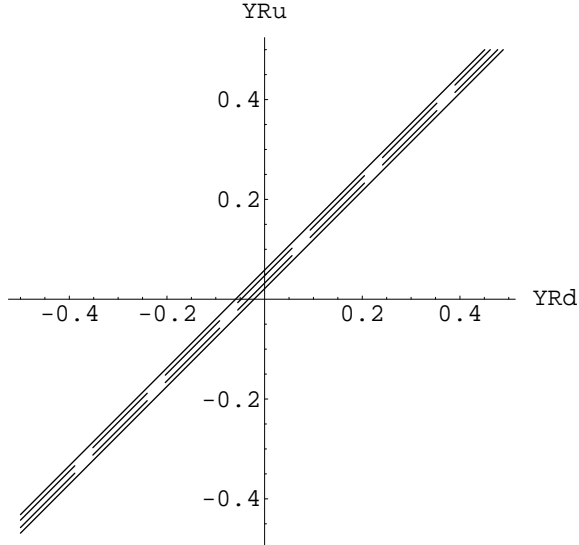


Figure 9: $\text{Re}(\epsilon'/\epsilon)$ as a function of Y_{Rd} and Y_{Ru} in the STC2 variant of Model 2. The 2σ and 5σ bands are the same as in Fig. 8.

Mixing and CP violation in the K^0 system constrained the ETC gauge boson masses to be so large that they do not contribute appreciably to any B -meson decays or mixing. Therefore, we focused on TC2 interactions in their standard (STC2) and flavor-universal (FUTC2) variants, working with $SU(3)_1$ and $U(1)_1$ couplings $\alpha_t(V_8)$ and $\alpha_t(Z')$ chosen large

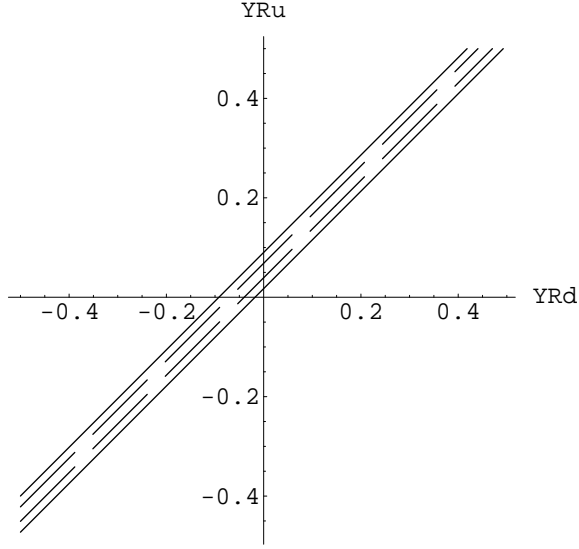


Figure 10: $\text{Re}(\epsilon'/\epsilon)$ as a function of Y_{Rd} and Y_{Ru} in the FUTC2 variant of Model 2. The 2σ and 5σ bands are the same as in Fig. 8.

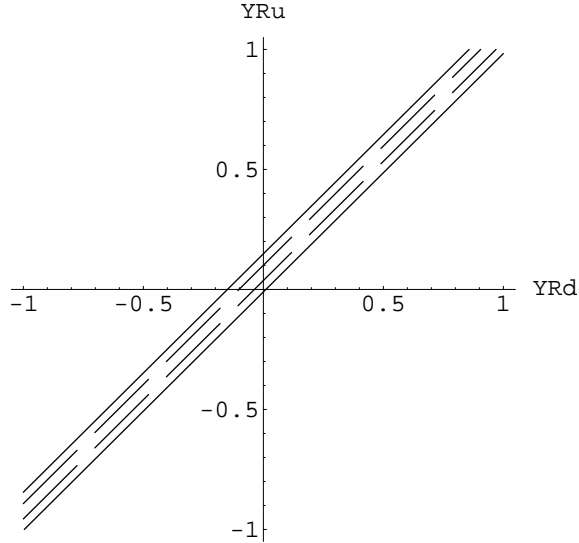


Figure 11: $\text{Re}(\epsilon'/\epsilon)$ as a function of Y_{Rd} and Y_{Ru} in the STC2 variant of Model 3. The 2σ and 5σ bands are the same as in Fig. 8.

enough to avoid their fine tuning. For each variant, we considered three models of the quark mass matrices with $\arg \det(M_q) = 0$, designed to give a fairly realistic CKM matrix, $V = U_L^\dagger D_L$, and various amounts of mixing in the D_R alignment matrix.

We found that B_d -mixing constraints require $M_{V8,Z'} \gtrsim 5\text{--}25\text{ TeV}$ even in models with a

non-block-diagonal D_R . These bounds are as higher than those found in Ref. [21] because of the larger value of $|V_{td}|$ used here. They are considerably higher than the $M_{Z'} \gtrsim 1$ TeV estimated in Ref. [22]. The principal reason for that disagreement is our insistence on using a large $U(1)_1$ coupling $\alpha_q(Z')$ to avoid fine-tuning $\alpha_q(V_8)$. But, we cannot win because the larger TC2 boson masses also require fairly severe fine tuning, at the level of 3%–0.05%. Future measurements of ΔM_{B_s} may cause the TC2 gauge boson mass limit to increase further, as we found that models with $M_{Z'} = M_{V_8} \cong 5$ TeV predict values for ΔM_{B_s} and x_s up to 15 times greater than the current experimental bound.

Employing a minimal renormalization scheme, we calculated the effect of TC2 interactions on $B_d \rightarrow XK_S$ decays. We found that both variants of TC2 can predict a $\sin 2\beta_{\text{eff}}$ discrepancy among $B_d \rightarrow XK_S$ modes. However, this discrepancy is directly related to the magnitudes and phase difference between D_{Rbq} and D_{Lbq} matrix elements, and thus is possible *only* for models with quark mass matrices with non-block-diagonal D_R (Models 2 and 3). In these models, we found that moderate Y_{Rd}, Y_{Ru} hypercharges are generally sufficient to achieve discrepancies consistent with the current experimental values.

The contributions from TC2 to $\text{Re}(\epsilon'/\epsilon)$ were also calculated and found to be significant, even for models with block-diagonal D_R . To accommodate the experimental value of $\text{Re}(\epsilon'/\epsilon)$ in the alignment models considered, we must have $Y_{Rd} \cong Y_{Ru}$. This further restricts the range of $\sin 2\beta$ values an individual alignment model can generate, especially in the FUTC2 variant, as can be seen from Figs. 1–7.

To sum up, new sources of flavor mixing and CP violation from TC2 interactions can be compatible with all constraints and still yield a discrepancy in the observable $\sin 2\beta_{\text{eff}}$. However, to accomplish this fit, the Z' and V_8 masses must be rather large so that TC2 interactions are fine-tuned at about the percent level. Somewhat surprisingly, TC2 effects also tend to produce large values for $\text{Re}(\epsilon'/\epsilon)$ and ΔM_{B_s} . We may have to wait till the end of this decade before we know the value of the latter.

Acknowledgements

We are especially indebted to Gustavo Burdman for tutoring K.L. in B -physics and early calculations of $\text{Re}(\epsilon'/\epsilon)$ and to Tonguç Rador and Estia Eichten for creating the suite of programs used for quark vacuum alignment. Our thanks also go to Sekhar Chivukula and Yuval Grossman for several helpful discussions.

Appendix A: ETC Gauge Boson Mass Scales

To set the ETC strengths $\Lambda^{TT}, \Lambda^{Tq}, \Lambda^{qq}$ in \mathcal{H}' of Eq. (4), we are assuming a TC2 model containing N identical electroweak doublets of technifermions. The technipion decay constant (which sets the technicolor energy scale) is then $F_T = F_\pi/\sqrt{N}$, where $F_\pi = 246$ GeV is the fundamental weak scale. We estimate the ETC masses in \mathcal{H}' by the rule stated in Sect. 3: The ETC scale M_{ETC}/g_{ETC} in a term involving weak eigenstates of the form $\bar{q}'_i q'_j \bar{q}'_j q'_i$ or $\bar{q}'_i q'_i \bar{q}'_j q'_j$ (for $q'_i = u'_i$ or d'_i) is approximately the same as the scale that generates the $\bar{q}'_{Ri} q'_{Lj}$ mass term, $(\mathcal{M}_q)_{ij}$.

The ETC gauge boson mass $M_{ETC}(q)$ giving rise to a quark mass $m_q(M_{ETC})$ — an element or eigenvalue of \mathcal{M}_q — is defined by [7]

$$m_q(M_{ETC}) \simeq \frac{g_{ETC}^2}{M_{ETC}^2(q)} \langle \bar{T}T \rangle_{ETC}. \quad (63)$$

Here, the quark mass and the technifermion bilinear condensate, $\langle \bar{T}T \rangle_{ETC}$, are renormalized at the scale $M_{ETC}(q)$. The condensate is related to the one renormalized at the technicolor scale $\Lambda_{TC} \simeq F_T$ by

$$\langle \bar{T}T \rangle_{ETC} = \langle \bar{T}T \rangle_{TC} \exp \left(\int_{\Lambda_{TC}}^{M_{ETC}(q)} \frac{d\mu}{\mu} \gamma_m(\mu) \right). \quad (64)$$

Scaling $\langle \bar{T}T \rangle_{TC}$ from QCD, we expect

$$\langle \bar{T}T \rangle_{TC} \equiv \Delta_T \simeq 4\pi F_T^3 = 4\pi F_\pi^3 / N^{3/2}. \quad (65)$$

The anomalous dimension γ_m of the operator $\bar{T}T$ is given in perturbation theory by

$$\gamma_m(\mu) = \frac{3C_2(R)}{2\pi} \alpha_{TC}(\mu) + O(\alpha_{TC}^2), \quad (66)$$

where $C_2(R)$ is the quadratic Casimir of the technifermion $SU(N_{TC})$ representation R . For the fundamental representation of $SU(N_{TC})$ to which we assume our technifermions T belong, it is $C_2(N_{TC}) = (N_{TC}^2 - 1)/2N_{TC}$. In a walking technicolor theory, however, the coupling $\alpha_{TC}(\mu)$ decreases very slowly from its critical chiral symmetry breaking value at Λ_{TC} , and $\gamma_m(\mu) \simeq 1$ for $\Lambda_{TC} \lesssim \mu \lesssim M_{ETC}$.

An accurate evaluation of the condensate enhancement integral in Eq. (64) requires detailed specification of the technicolor model and knowledge of the $\beta(\alpha_{TC})$ -function for large coupling.²⁸ Lacking this, we estimate the enhancement by assuming that

$$\gamma_m(\mu) = \begin{cases} 1 & \text{for } \Lambda_{TC} < \mu < \mathcal{M}_{ETC}/\kappa \\ 0 & \text{for } \mu > \mathcal{M}_{ETC}/\kappa \end{cases} \quad (67)$$

²⁸See Ref. [49] for an attempt to calculate this integral in a walking technicolor model.

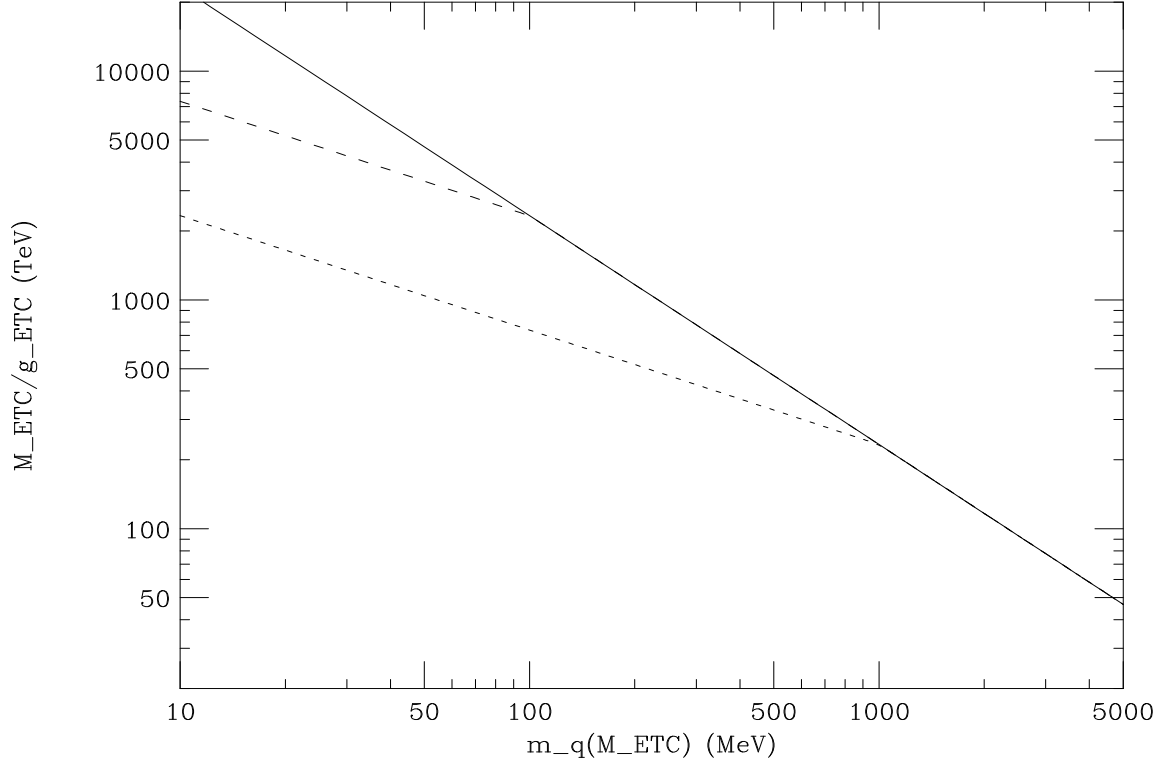


Figure 12: Extended technicolor scale M_{ETC}/g_{ETC} as a function of quark mass m_q renormalized at M_{ETC} for $\kappa = 1$ (solid curve), 10 (dashed), and 100 (solid).

Here, \mathcal{M}_{ETC} is the largest ETC scale, i.e., the one generating the smallest term in the quark mass matrix for $\kappa = 1$. The parameter $\kappa > 1$ parameterizes the departure from the strict walking limit (which we characterize by $\gamma_m = 1$ up to \mathcal{M}_{ETC}/κ). Then, using Eqs. (63,64), we obtain

$$\frac{M_{ETC}(q)}{g_{ETC}} = \begin{cases} \frac{\sqrt{64\pi^3\alpha_{ETC}} F_\pi^2}{Nm_q} & \text{if } M_{ETC}(q) < \mathcal{M}_{ETC}/\kappa \\ \sqrt{\frac{4\pi\mathcal{M}_{ETC}F_\pi^2}{\kappa Nm_q}} & \text{if } M_{ETC}(q) > \mathcal{M}_{ETC}/\kappa \end{cases} \quad (68)$$

To evaluate this, we take $\alpha_{ETC} = 3/4$, a moderately strong value as would be expected in walking technicolor, $N = 10$, a typical number of doublets in TC2 models with topcolor breaking (see, e.g., Ref. [16]). Then, taking the smallest quark mass at the ETC scale to be 10 MeV, we find $\mathcal{M}_{ETC} = 7.17 \times 10^4$ TeV. The resulting estimates of M_{ETC}/g_{ETC} are plotted in Fig. 12 for $\kappa = 1, 10$, and 100. They run from $M_{ETC}/g_{ETC} = 47$ TeV for $m_q = 5$ GeV to $2.34/\sqrt{\kappa} \times 10^4$ TeV/ for $m_q = 10$ MeV. Very similar results are obtained for $\alpha_{ETC} = 1/2$ and $N = 8$: $M_{ETC}/g_{ETC} = 48$ TeV for $m_q = 5$ GeV to $2.38/\sqrt{\kappa} \times 10^4$ TeV/ for $m_q = 10$ MeV.

Appendix B: Three Mass Models and their Alignment Matrices

In Sect. 2 we described a scenario for solving the strong CP problem of QCD. Briefly, it was based on the natural appearance of vacuum-aligning phases in the technicolor sector which are rational multiples of π *and* the assumption that ETC interactions map these phases onto the primordial quark mass matrix \mathcal{M}_q of Eq. (12) in such a way that

$$\arg \det(\mathcal{M}_q) \equiv \arg \det(\mathcal{M}_u) + \arg \det(\mathcal{M}_d) = 0. \quad (69)$$

Since \mathcal{M}_q in this case is brought to real, positive, diagonal form M_q by unimodular matrices $Q_{L,R} = (U, D)_{L,R}$, then $\arg \det(M_q) = 0$ also. In the absence of an explicit ETC model, we cannot construct \mathcal{M}_q from “first principles”. In this appendix, therefore, we write down mass matrices with rational phases satisfying Eq. (69), carry out vacuum alignment in the quark sector by minimizing the energy $E_{Tq}(Q = Q_L Q_R^\dagger) \cong -\text{Tr}(\mathcal{M}_q Q + \text{h.c.}) \Delta_q(M_{ETC})$, and thus determine the aligning matrices $Q_{L,R}$, and the CKM matrix $V = U_L^\dagger D_L$ with its unphysical phases removed.²⁹ We remind the reader that these \mathcal{M}_q have not been “fine-tuned” to give $|V_{uid_j}|$ in complete accord with values found in Ref. [34]

Mass Model 1: Block-Diagonal D_R

As we discussed in Sect. 2, there is an argument, albeit one we believe is questionable, that \mathcal{M}_d must have a nearly triangular texture to suppress B_d – \bar{B}_d mixing induced by bottom pions. That texture is needed to make $|D_{Rbd}| \ll |D_{Lbd}|$. This model has such a primordial \mathcal{M}_d . Then, because the very large TC2 contribution to $(\mathcal{M}_u)_{tt}$ makes mixing angles between u, c and t very small, all mixing between the heavy and light generations in this model occurs in D_L . To create small m_u and m_d while having a large CKM angle $\theta_{12} \simeq 0.2$, we take mass matrices with a seesaw structure:

$$\begin{aligned} \mathcal{M}_u(M_{ETC}) &= \begin{pmatrix} (0, 0) & (200, 0) & (0, 0) \\ (16, 2\pi/3) & (900, 0) & (0, 0) \\ (0, 0) & (0, 0) & (160000, 0) \end{pmatrix}; \\ \mathcal{M}_d(M_{ETC}) &= \begin{pmatrix} (0, 0) & (20, -\pi/3) & (0, 0) \\ (22, 0) & (100, 0) & (0, 0) \\ (17, 0) & (145, -\pi/3) & (3500, -\pi/3) \end{pmatrix}. \end{aligned} \quad (70)$$

The notation is $(|(\mathcal{M}_q)_{ij}|, \arg((\mathcal{M}_q)_{ij}))$, with masses in MeV, and these matrices are renormalized at $M_{ETC} \sim 10^3$ TeV. The quark mass eigenvalues extracted from \mathcal{M}_q are:

$$\begin{aligned} m_u &= 3.47, \quad m_c = 922, \quad m_t = 160000; \\ m_d &= 4.22, \quad m_2 = 104, \quad m_b = 3503. \end{aligned} \quad (71)$$

²⁹The programs to carry out quark-sector vacuum alignment were developed by Tonguç Rador in 2000.

Quark masses at the EW scale will be enhanced by QCD and, possibly, TC2 renormalizations which we will not carry out. For the calculations in Sects. 4–7, we took quark masses from Ref. [34].

The $U(3)$ matrices $U = U_L U_R^\dagger$ and $D = D_L D_R^\dagger$ obtained by minimizing the vacuum energy E_{T_q} are:

$$U = \begin{pmatrix} (0.972, \pi/3) & (0.233, -2\pi/3) & (0, 0) \\ (0.233, 0) & (0.972, 0) & (0, 0) \\ (0, 0) & (0, 0) & (1.000, 0) \end{pmatrix};$$

$$D = \begin{pmatrix} (0.922, -2\pi/3) & (0.387, 0) & (0.0047, 0.014\pi) \\ (0.387, \pi/3) & (0.921, 0) & (0.0402, \pi/3) \\ (0.0141, -0.755\pi) & (0.0379, -0.986\pi) & (0.999, \pi/3) \end{pmatrix};$$

The minimization routine we use must determine the 6×6 block-diagonal $Q = (U, D)$ all at once because it, not U and D separately, is unimodular. It is obvious that large elements of U and D have phases which are rational multiples of π , reflecting those in \mathcal{M}_u and \mathcal{M}_d . But the program has a little difficulty determining precisely the phases for small matrix elements. For example, the phase 0.014π of D_{db} is probably zero. We do not believe there are large errors in any of the phases in these matrices. Therefore, the observable combinations of phases in $V = U_L^\dagger D_L$ and $Q_{L,R}$ below should be well-determined.

By Nuyts' theorem [32], the mass matrix $\mathcal{M}_q Q$ which minimizes the vacuum energy is diagonalized by the single block-diagonal $SU(6)$ matrix $Q_R = (U, D)_R$. With Q and Q_R determined, we obtain $Q_L = Q Q_R$ and $M_q = Q_R^\dagger \mathcal{M}_q Q_L$. We then construct V and remove its five unobservable phases to put it in the standard form, Eq. (16). This leaves $2 \times 6 - 1 - 5 = 6$ independent phases in the Q_L . To maintain the vacuum's alignment, these five q_{Li} phase changes must be accompanied by the same transformations on the q_{Ri} . No further quark phase changes are permissible, leaving Q_R with 11 independent phases. One of these is the overall T_{R3} angle, $\arg \det(D_R) = -\arg \det(U_R)$. Only the remaining 10 Q_R -phases, five each in U_R and D_R , appear in the right-handed flavor ETC and TC2 currents and are, in principle, measurable.

The phase-adjusted CKM matrix is:

$$V = \begin{pmatrix} (0.976, 0) & (0.216, 0) & (0.0045, -0.977) \\ (0.216, 3.142) & (0.976, 0) & (0.0415, 0) \\ (0.0075, -0.516) & (0.0410, 3.161) & (0.999, 0) \end{pmatrix}. \quad (72)$$

The angles θ_{ij} and phase δ_{13} corresponding to this matrix are:

$$\theta_{12} = 0.218, \quad \theta_{23} = 0.0415, \quad \theta_{13} = 0.00455, \quad \delta_{13} = 0.977. \quad (73)$$

The magnitudes of the $V_{u_i d_j}$ are in fair agreement with those in Ref. [34]. The phase-adjusted

$Q_{L,R}$ matrices are (up to terms of $\mathcal{O}(10^{-5})$):

$$\begin{aligned}
U_L &= \begin{pmatrix} (1.000, 0.291) & (0.017, -1.867) & (0, 0) \\ (0.017, -0.756) & (1.000, 0.227) & (0, 0) \\ (0, 0) & (0, 0) & (1.000, 0.225) \end{pmatrix}; \\
D_L &= \begin{pmatrix} (0.978, 0.294) & (0.207, 0.224) & (0.0049, -0.821) \\ (0.207, 3.435) & (0.977, 0.224) & (0.041, 0.225) \\ (0.0074, -0.291) & (0.041, 3.387) & (0.999, 0.225) \end{pmatrix}; \\
U_R &= \begin{pmatrix} (0.976, -0.756) & (0.217, 0.227) & (0, 0) \\ (0.216, 2.385) & (0.976, 0.227) & (0, 0) \\ (0, 0) & (0, 0) & (1, 0.225) \end{pmatrix}; \\
D_R &= \begin{pmatrix} (0.982, 2.388) & (0.188, -0.824) & (2.4 \times 10^{-4}, -0.822) \\ (0.188, 0.294) & (0.982, 0.223) & (0.0012, 0.203) \\ (0, 0) & (0.0012, 2.34) & (1.000, -0.822) \end{pmatrix}.
\end{aligned} \tag{74}$$

By design, D_R is very nearly block diagonal.

Mass Model 2: Nontrivial D_R

This model has nonzero heavy-light generational mixing in D_R . Elements are again of the form $(|(\mathcal{M}_q)_{ij}|, \arg((\mathcal{M}_q)_{ij}))$:

$$\begin{aligned}
\mathcal{M}_u(M_{ETC}) &= \begin{pmatrix} (0, 0) & (200, 0) & (0, 0) \\ (16, 2\pi/3) & (900, 0) & (0, 0) \\ (0, 0) & (0, 0) & (160000, 0) \end{pmatrix}; \\
\mathcal{M}_d(M_{ETC}) &= \begin{pmatrix} (0, 0) & (20, -\pi/3) & (0, 0) \\ (22, 0) & (100, 0) & (140, -\pi/3) \\ (17, 0) & (100, -\pi/3) & (3500, -\pi/3) \end{pmatrix}.
\end{aligned} \tag{75}$$

The primordial mass matrices in Model 2 are similar to those of Model 1, except that the off-diagonal elements $(\mathcal{M}_d)_{bs}$ and $(\mathcal{M}_d)_{sb}$ are comparable. For this reason, the physical masses of Model 2 are practically identical to those of Model 1, but we will not obtain a block-diagonal D_R . The matrices U, D minimizing the vacuum energy are:

$$\begin{aligned}
U &= \begin{pmatrix} (0.972, \pi/3) & (0.233, -2\pi/3) & (0, 0) \\ (0.233, 0) & (0.972, 0) & (0, 0) \\ (0, 0) & (0, 0) & (1.000, 0) \end{pmatrix}; \\
D &= \begin{pmatrix} (0.921, -0.655\pi) & (0.388, 0) & (0.010, -0.996\pi) \\ (0.388, \pi/3) & (0.921, -0.011\pi) & (0.0334, 0.727\pi) \\ (0.0097, -0.794\pi) & (0.0336, 0.566\pi) & (0.999, \pi/3) \end{pmatrix};
\end{aligned}$$

The phase-adjusted CKM matrix is:

$$V = \begin{pmatrix} (0.977, 0) & (0.214, 0) & (0.0049, 5.259) \\ (0.214, 3.142) & (0.976, 0) & (0.0292, 0) \\ (0.0055, -0.826) & (0.0290, 3.172) & (1.000, 0) \end{pmatrix}. \quad (76)$$

The corresponding angles θ_{ij} and phase δ_{13} are:

$$\theta_{12} = 0.216, \quad \theta_{23} = 0.0292, \quad \theta_{13} = 0.00489, \quad \delta_{13} = 1.024. \quad (77)$$

The most important features of Model 2 are the size of the CKM element $|V_{td}| = 0.0055$, $|V_{ts}| = 0.029$ compared to $|V_{td}| = 0.0075$, $|V_{ts}| = 0.041$ in Model 1. The smaller $|V_{td}|$ is, the lighter their Z' and V_8 can be while still complying with the constraints from B_d mixing. Lighter gauge bosons then lead to larger TC2 contributions to decay and mixing processes. The CKM element $|V_{ts}|$ in Model 2 is only $\sim 70\%$ of the value in Ref. [34], which is known by the unitarity relation $|V_{ts}| \cong |V_{cb}| \cong 0.040$. The calculation of ΔM_{B_s} is affected the most by this discrepancy as explained in Section 7.2.

The phase-adjusted alignment matrices are:

$$\begin{aligned} U_L &= \begin{pmatrix} (1.000, -1.842) & (0.019, -4.035) & (0, 0) \\ (0.0169, -2.889) & (1.000, -1.941) & (0, 0) \\ (0, 0) & (0, 0) & (1.000, -1.909) \end{pmatrix}; \\ D_L &= \begin{pmatrix} (0.979, -1.839) & (0.205, -1.908) & (0.0051, 3.328) \\ (0.205, 1.267) & (0.978, -1.944) & (0.029, -1.943) \\ (0.0055, 3.548) & (0.0290, 1.263) & (0.999, -1.909) \end{pmatrix}; \\ U_R &= \begin{pmatrix} (0.976, -2.889) & (0.217, -1.941) & (0, 0) \\ (0.217, 0.252) & (0.976, -1.941) & (0, 0) \\ (0, 0) & (0, 0) & (1, -1.909) \end{pmatrix}; \\ D_R &= \begin{pmatrix} (0.981, 0.220) & (0.192, 3.292) & (1.6 \times 10^{-4}, 3.293) \\ (0.191, -1.839) & (0.981, -1.908) & (0.040, 3.344) \\ (0.0077, 1.303) & (0.0397, 1.215) & (0.999, 3.327) \end{pmatrix}. \end{aligned} \quad (78)$$

Note that $|D_{Rbq}|$ is actually larger than $|D_{Lbq}|$ for $q = d, s$.

Mass Model 3: Nontrivial D_R with $|D_{Rbq}| \simeq |D_{Lbq}|$

This model also has a nontrivial heavy-light generational mixing in D_R , but we start from a more symmetric \mathcal{M}_d than in Mass Model 2:

$$\begin{aligned}\mathcal{M}_u(M_{ETC}) &= \begin{pmatrix} (0,0) & (200,0) & (0,0) \\ (16,2\pi/3) & (900,0) & (0,0) \\ (0,0) & (0,0) & (160000,0) \end{pmatrix}; \\ \mathcal{M}_d(M_{ETC}) &= \begin{pmatrix} (0,0) & (20,-\pi/3) & (0,0) \\ (22,0) & (100,0) & (100,-\pi/3) \\ (17,0) & (100,-\pi/3) & (3500,-\pi/3) \end{pmatrix}.\end{aligned}\tag{79}$$

The physical masses at M_{ETC} are again almost identical to those of Model 1. The minimizing matrices U, D are:

$$\begin{aligned}U &= \begin{pmatrix} (0.972, \pi/3) & (0.233, -2\pi/3) & (0,0) \\ (0.233, 0) & (.972, 0) & (0,0) \\ (0,0) & (0,0) & (1.000, 0) \end{pmatrix}; \\ D &= \begin{pmatrix} (0.922, -0.659\pi) & (0.388, 0) & (0.0061, -0.993\pi) \\ (0.388, \pi/3) & (0.921, -0.008\pi) & (0.0273, 0.640\pi) \\ (0.0096, -0.796\pi) & (0.0263, 0.659\pi) & (0.999, \pi/3) \end{pmatrix};\end{aligned}$$

The CKM matrix in standard form is:

$$V = \begin{pmatrix} (0.977, 0) & (0.215, 0) & (0.0048, -1.023) \\ (0.215, 3.142) & (0.976, 0) & (0.0290, 0) \\ (0.0055, -0.816) & (0.0289, 3.172) & (1.000, 0) \end{pmatrix}.\tag{80}$$

Its angles θ_{ij} and phase δ_{13} are

$$\theta_{12} = 0.216, \quad \theta_{23} = 0.0290, \quad \theta_{13} = 0.00482, \quad \delta_{13} = 1.023.\tag{81}$$

Like Mass Model 2, this model has a small CKM V_{td} element. We therefore expect lower Z' and V_8 mass bounds than in Model 1. That is indeed the case, but they are somewhat larger than in Model 2. This demonstrates the difficulty of obtaining model-independent lower bounds on M_{Z', V_8} from the B_d -mixing constraint with non-block diagonal D_R — a situation already emphasized by Simmons [22].

The phase-adjusted $Q_{L,R}$ are:

$$\begin{aligned}
U_L &= \begin{pmatrix} (1.000, -1.891) & (0.017, -4.074) & (0, 0) \\ (0.017, -2.939) & (1.000, -1.980) & (0, 0) \\ (0, 0) & (0, 0) & (1.000, -1.958) \end{pmatrix} ; \\
D_L &= \begin{pmatrix} (0.979, -1.889) & (0.205, -1.958) & (0.0050, 3.278) \\ (0.205, 1.228) & (0.978, -1.983) & (0.0289, -1.983) \\ (0.0055, 3.509) & (0.0289, 1.214) & (1.000, -1.958) \end{pmatrix} ; \\
U_R &= \begin{pmatrix} (0.976, -2.939) & (0.217, -1.980) & (0, 0) \\ (0.217, 0.203) & (0.976, -1.980) & (0, 0) \\ (0, 0) & (0, 0) & (1.000, -1.958) \end{pmatrix} ; \\
D_R &= \begin{pmatrix} (0.982, 0.181) & (0.190, 3.253) & (1.6 \times 10^{-4}, 3.253) \\ (0.190, -1.888) & (0.981, -1.958) & (0.0290, 3.302) \\ (0.0054, 1.254) & (0.0285, 1.158) & (1.000, 3.278) \end{pmatrix} . \tag{82}
\end{aligned}$$

The effect of the more symmetric \mathcal{M}_d is seen in the (bd) and (bs) elements of D_L and D_R .

References

- [1] T. E. Browder, “Results on the CKM angle $\phi(1)(\beta)$,” hep-ex/0312024.
- [2] **BABAR** Collaboration, B. Aubert *et. al.*, “Measurements of CP asymmetries in the decay $B \rightarrow \bar{\ell} \Phi K$,” hep-ex/0408072.
- [3] **BELLE** Collaboration, K. Abe *et. al.*, “New measurements of time-dependent CP-violating asymmetries in $b \rightarrow \bar{\ell} s$ transitions at Belle,” hep-ex/0409049.
- [4] **BABAR** Collaboration, B. Aubert *et. al.*, “Measurements of CP-violating asymmetries and branching fractions in B meson decays to $\eta' K$,” *Phys. Rev. Lett.* **91** (2003) 161801, hep-ex/0303046.
- [5] **BABAR** Collaboration, B. Aubert *et. al.*, “Measurements of CP violating asymmetries in $B^0 \rightarrow K_S^0 \pi^0$ decays,” hep-ex/0403001.
- [6] C. T. Hill and E. H. Simmons, “Strong dynamics and electroweak symmetry breaking,” *Physics Reports* **381** (2003) 235–402, hep-ph/0203079.
- [7] K. Lane, “Two lectures on technicolor,” hep-ph/0202255. Lectures at l’Ecole de GIF, Annecy-le-Vieux, France, September 10–14, 2001.
- [8] E. Eichten and K. Lane, “Dynamical breaking of weak interaction symmetries,” *Phys. Lett.* **B90** (1980) 125–130.
- [9] B. Holdom, “Raising the sideways scale,” *Phys. Rev.* **D24** (1981) 1441.
- [10] T. W. Appelquist, D. Karabali, and L. C. R. Wijewardhana, “Chiral hierarchies and the flavor changing neutral current problem in technicolor,” *Phys. Rev. Lett.* **57** (1986) 957.
- [11] K. Yamawaki, M. Bando, and K.-i. Matumoto, “Scale invariant technicolor model and a technidilaton,” *Phys. Rev. Lett.* **56** (1986) 1335.
- [12] T. Akiba and T. Yanagida, “Hierarchic chiral condensate,” *Phys. Lett.* **B169** (1986) 432.
- [13] C. T. Hill, “Topcolor assisted technicolor,” *Phys. Lett.* **B345** (1995) 483–489, hep-ph/9411426.
- [14] R. S. Chivukula and H. Georgi, “Effective field theory of vacuum tilting,” *Phys. Rev.* **D58** (1998) 115009, hep-ph/9806289.
- [15] R. S. Chivukula and J. Terning, “Precision electroweak constraints on topcolor-assisted technicolor,” *Phys. Lett.* **B385** (1996) 209–217, hep-ph/9606233.

- [16] K. Lane, “Symmetry breaking and generational mixing in topcolor-assisted technicolor,” *Phys. Rev.* **D54** (1996) 2204–2212, hep-ph/9602221.
- [17] R. S. Chivukula, A. G. Cohen, and E. H. Simmons, “New strong interactions at the Tevatron?,” *Phys. Lett.* **B380** (1996) 92–98, hep-ph/9603311.
- [18] M. B. Popovic and E. H. Simmons, “A heavy top quark from flavor-universal colorons,” *Phys. Rev.* **D58** (1998) 095007, hep-ph/9806287.
- [19] K. Lane, “ $K^0-\bar{K}^0$ and $B^0-\bar{B}^0$ constraints on technicolor,” hep-ph/0106279. Invited talk at Les Rencontres de Physique de la Vallée d’Aoste, La Thuile, Italy, March 4-10, 2001.
- [20] K. Lane, “Strong and weak CP violation in technicolor,” hep-ph/0106328. Invited talk at the Eighth International Symposium on Particles, Strings and Cosmology—PASCOS 2001, University of North Carolina, Chapel Hill, NC, April 10–15, 2001.
- [21] G. Burdman, K. D. Lane, and T. Rador, “ $\bar{B}-B$ mixing constrains topcolor-assisted technicolor,” *Phys. Lett.* **B514** (2001) 41–46, hep-ph/0012073.
- [22] E. H. Simmons, “Limitations of B meson mixing bounds on technicolor theories,” *Phys. Lett.* **B526** (2002) 365–369, hep-ph/0111032.
- [23] G. Burdman, “Flavor violation in warped extra dimensions and CP asymmetries in B decays,” hep-ph/0310144.
- [24] R. F. Dashen, “Some features of chiral symmetry breaking,” *Phys. Rev.* **D3** (1971) 1879–1889.
- [25] E. Eichten, K. Lane, and J. Preskill, “CP violation without elementary scalar fields,” *Phys. Rev. Lett.* **45** (1980) 225.
- [26] K. Lane, “CP nonconservation in dynamically broken gauge theories,” *Phys. Scripta* **23** (1981) 1005.
- [27] K. Lane, T. Rador, and E. Eichten, “Vacuum alignment in technicolor theories. I: The technifermion sector,” *Phys. Rev.* **D62** (2000) 015005, hep-ph/0001056.
- [28] M. E. Peskin and T. Takeuchi, “A new constraint on a strongly interacting Higgs sector,” *Phys. Rev. Lett.* **65** (1990) 964–967.
- [29] B. Holdom and J. Terning, “Large corrections to electroweak parameters in technicolor theories,” *Phys. Lett.* **B247** (1990) 88–92.
- [30] M. Golden and L. Randall, “Radiative corrections to electroweak parameters in technicolor theories,” *Nucl. Phys.* **B361** (1991) 3–23.

- [31] R. D. Peccei, “QCD, strong CP and axions,” *J. Korean Phys. Soc.* **29** (1996) S199–S208, hep-ph/9606475.
- [32] J. Nuyts, “Is CP-invariance violation caused by an SU(3) singlet?,” *Phys. Rev. Lett.* **26** (1971) 1604–1605.
- [33] H. Harari and M. Leurer, “Recommending a standard choice of Cabibbo angles and KM phases for any number of generations,” *Phys. Lett.* **B181** (1986) 123.
- [34] **Particle Data Group** Collaboration, S. Eidelman *et. al.*, “Review of particle physics,” *Phys. Lett.* **B592** (2004) 1.
- [35] G. Buchalla, G. Burdman, C. T. Hill, and D. Kominis, “GIM violation and new dynamics of the third generation,” *Phys. Rev.* **D53** (1996) 5185–5200, hep-ph/9510376.
- [36] D. Kominis, “Flavor changing neutral current constraints in topcolor assisted technicolor,” *Phys. Lett.* **B358** (1995) 312–317, hep-ph/9506305.
- [37] K. Lane and E. Eichten, “Natural topcolor assisted technicolor,” *Phys. Lett.* **B352** (1995) 382–387, hep-ph/9503433.
- [38] K. Lane, “A new model of topcolor-assisted technicolor,” *Phys. Lett.* **B433** (1998) 96–101, hep-ph/9805254.
- [39] A. J. Buras, “Flavor dynamics: CP violation and rare decays,” hep-ph/0101336.
- [40] A. J. Buras and R. Fleischer, “Quark mixing, CP violation and rare decays after the top quark discovery,” *Adv. Ser. Direct. High Energy Phys.* **15** (1998) 65–238, hep-ph/9704376.
- [41] G. Kramer, W. F. Palmer, and H. Simma, “CP violation and strong phases from penguins in $B^{+-} \rightarrow P P$ and $B^{+-} \rightarrow V P$ decays,” *Z. Phys.* **C66** (1995) 429–438, hep-ph/9410406.
- [42] Y. Grossman, G. Isidori, and M. P. Worah, “CP asymmetry in $B/d \rightarrow \ell^+ \ell^- \Phi K(S)$: Standard model pollution,” *Phys. Rev.* **D58** (1998) 057504, hep-ph/9708305.
- [43] G. Buchalla, A. J. Buras, and M. E. Lautenbacher, “Weak decays beyond leading logarithms,” *Rev. Mod. Phys.* **68** (1996) 1125–1144, hep-ph/9512380.
- [44] A. Ali, G. Kramer, and C.-D. Lu, “Experimental tests of factorization in charmless nonleptonic two-body B decays,” *Phys. Rev.* **D58** (1998) 094009, hep-ph/9804363.
- [45] A. Ali and C. Greub, “An analysis of two-body nonleptonic B decays involving light mesons in the standard model,” *Phys. Rev.* **D57** (1998) 2996–3016, hep-ph/9707251.

- [46] R. Fleischer, “CP violation in the B system and relations to $K \rightarrow \pi\nu\bar{\nu}$ decays,” *Phys. Rept.* **370** (2002) 537–680, hep-ph/0207108.
- [47] A. J. Buras and M. Jamin, “Epsilon’/epsilon at the NLO: 10 years later,” *JHEP* **01** (2004) 048, hep-ph/0306217.
- [48] A. J. Buras and J.-M. Gerard, “What is the (epsilon’/epsilon)(exp) telling us?,” *Phys. Lett.* **B517** (2001) 129–134, hep-ph/0106104.
- [49] K. D. Lane and M. V. Ramana, “Walking technicolor signatures at hadron colliders,” *Phys. Rev.* **D44** (1991) 2678–2700.